frontiers | Frontiers in Environmental Science

TYPE Original Research
PUBLISHED 20 May 2024
DOI 10.3389/fenvs.2024.1376443

OPEN ACCESS

EDITED BY
Daniel D. Snow,
University of Nebraska-Lincoln, United States

REVIEWED BY
Banajarani Panda,
Ravenshaw University, India
Jeff Westrop,
University of Nebraska-Lincoln, United States

*CORRESPONDENCE
Ping Wang,
wangping@igsnrr.ac.cn
Shiqi Liu,
liusq@igsnrr.ac.cn

RECEIVED 25 January 2024
ACCEPTED 26 April 2024
PUBLISHED 20 May 2024

CITATION
Zhang J, Wang P, Liu S and Yu J (2024), Mechanism controlling groundwater chemistry in the hyper-arid basin with intermittent river flow: insights from long-term observations (2001–2023) in the lower Heihe River, Northwest China.
Front. Environ. Sci. 12:1376443.
doi: 10.3389/fenvs.2024.1376443

Mechanism controlling groundwater chemistry in the hyper-arid basin with intermittent river flow: insights from long-term observations (2001–2023) in the lower Heihe River, Northwest China

Jialing Zhang[1,2], Ping Wang[1,2]*, Shiqi Liu[1]* and Jingjie Yu[1,2]

[1]Key Laboratory of Water Cycle and Related Land Surface Processes, Institute of Geographic Sciences and Natural Resources Research, Chinese Academy of Sciences, Beijing, China, [2]College of Resources and Environment, University of Chinese Academy of Sciences, Beijing, China

The geochemical processes of groundwater in arid regions are generally influenced by both natural hydrological processes and human activities. However, impacts of water-rock interactions on groundwater recharge via hydrological processes, controlled by both intermittent river water flow and groundwater withdrawals, is still poorly understood. In this study, 327 groundwater chemistry datasets collected from the upper, middle (including Gobi and riparian zones), and lower regions of the Ejina Delta in Northwest China from 2001 to 2023 were analyzed. Our results revealed that the total dissolved solids (*TDS*) concentration of groundwater in Ejina Delta ranged from approximately 881.5 ± 331.6 mg/L in the upper regions to 1,953.6 ± 1,208.5 mg/L in the lower regions, with an increasing trend observed. Ecological water conveyance (*EWC*), recharging aquifer through intermittent river water flow, resulted in a decrease in *TDS* concentrations from 2001 to 2023 mainly in the upper region. While irrigation notably affected groundwater chemistry in the lower region, resulting in a substantial increase in groundwater salinity. Groundwater chemistry in the Middle Gobi region remained relatively stable over the study period. Generally, the hydrochemical composition shifted from the Na-Mg-SO_4-HCO_3 and Na-Mg-Ca-SO_4-HCO_3 types in the upper region to Na-Mg-SO_4-HCO_3 and Na-Mg-SO_4-Cl types in the lower region, with Na-SO_4-Cl predominant in the Middle Gobi. These shifts were likely be attributed to the interplay of water-rock interactions, coupled with evaporation-crystallization processes. Inverse modeling using PHREEQC revealed that in the upper-middle region, primary water-rock interactions involved calcite dissolution and the precipitation of dolomite, gypsum, halite, and sylvite salts, as well as cation exchange reactions ($2NaX+Ca^{2+}\rightarrow CaX_2+2Na^{+}$). In contrast, the hydrogeological system in the middle-lower region exhibited an opposite pattern of water-rock interactions. Overall, ecological water conveyance partially facilitated water-rock interactions

during lateral groundwater flow, while irrigation disrupted the natural hydrogeochemical equilibrium, involving halite dissolution and opposite cation exchange reactions compared to other regions.

KEYWORDS

groundwater hydrochemistry, Ejina Delta, conceptual model, water-rock interaction, human activities

Highlights

- Groundwater salinity demonstrated an upward trend along the flow paths.
- Groundwater chemistry is influenced by river infiltration, evaporation, and human activities.
- Water-rock interactions control groundwater chemistry, with spatial variations.

1 Introduction

Due to the limited precipitation and high potential evaporation prevalent in endorheic basins within arid and semi-arid regions, a discernible reduction in water storage has emerged (Wang et al., 2018; Petch et al., 2023; Wan et al., 2023). Within these basins, groundwater plays a crucial role as a vital source for drinking water, social-economic developments, and the sustenance of natural ecosystems (Wang et al., 2011b; Yu et al., 2017; Wang T. et al., 2023). Notably, a widespread decline in groundwater levels in arid zones has been documented in the United States, China, and Australia (Scanlon et al., 2006; Döll et al., 2012; Famiglietti, 2014; Liu M. et al., 2018), leading to land desertification (Wang X. et al., 2022; Wang X. et al., 2023; Huang and Zhai, 2023; Yang et al., 2023) and ecological degradation (Wang and Cheng, 1999; Yu et al., 2022; Chen et al., 2023), which cause an increasing focus on groundwater research around the world. Through the analysis of the impact of geochemical processes on groundwater in the semi-arid regions of southern India, Karunanidhi et al. (2020) identified geological factors, agricultural irrigation, and industrial activities as key determinants of groundwater chemistry. Rajmohan et al. (2021) employed inverse geochemical modeling to simulate the saturation of minerals in groundwater, and revealed the impact of evaporation on groundwater salinity in the arid coastal aquifers of western Saudi Arabia. To enhance ecological and social sustainability in arid regions, it is of utmost importance to gain a comprehensive understanding of groundwater recharge and replenishment processes with hydrological models (Wang et al., 2013; Yao et al., 2015; Mensah et al., 2022), with particular attention to the exchanges between groundwater and ephemeral streams (Wang et al., 2017; Wang J. et al., 2023).

Naturally, the chemical composition of groundwater is governed by the foundational trio of atmospheric precipitation, rock dominance, and evaporation-crystallization processes (Gibbs, 1970; Marandi and Shand, 2018), as well as the additional influential factors such as ion exchange and microbial redox reactions (Labarca and Borquez, 2020; Qin et al., 2021). Additionally, beyond natural factors such as aquifer lithology, groundwater chemistry is significantly influenced by the chemical compositions of recharging water sources, groundwater velocity, and interactions with other water bodies or aquifers (Helena et al., 2000; Wang Y. et al., 2023). Consequently, an analysis of groundwater chemistry has the capability to detect surface-subsurface hydrological processes and the interactions between water and its surrounding environment (Liu et al., 2021; Wang et al., 2024). Previous studies have shown that groundwater in dry endorheic basins undergoes salinization processes primarily driven by rock dominance and evaporation-crystallization (Sami, 1992; Wen et al., 2005; Meredith et al., 2009; Wang W. et al., 2023). Moreover, other hydrochemical processes, such as simple mixing and ion exchange, can be observed in riparian areas, influenced by exchanges between river water and groundwater (Qin et al., 2012; Wang et al., 2013; Yuan et al., 2020).

All of the three largest endorheic rivers in northwestern China, the Tarim River (Tao et al., 2011; Qian et al., 2024), Heihe River (Akiyama et al., 2007; Cheng et al., 2014; Yu et al., 2023) and Shiyang River (Ma et al., 2005; Huo et al., 2008; Fang et al., 2022), are suffering from water deficits and riparian ecosystem crisis (Li et al., 2018; Chen et al., 2022). In this context, surface water replenishment under ecological water conveyance (*EWC*) leads to a reduction in water table depth (*WTD*), thereby facilitating the exchange between lower salinity surface water and groundwater, which effectively diminishes groundwater salinity and improves groundwater quality (Tao et al., 2008; Yuan et al., 2022). A comprehensive understanding of the hydrological cycle and the evolution of associated water chemistry holds fundamental importance for effective water resource managements and ecological restoration in these endorheic river basins (Li et al., 2018; Guo et al., 2019). Previously, the hydrochemical characteristics of river water and groundwater (Yang et al., 2011), as well as the evolution of groundwater chemistry (Zhu et al., 2008) in endorheic rivers of northwestern China, have been determined through the analysis of groundwater samples collected over relatively short time periods. However, comprehension of the long-term changes in groundwater chemistry and the driving mechanisms behind these changes remains limited.

The shallow aquifer of the Ejina Delta is predominantly recharged by the Heihe River (Wang et al., 2011a). The depth of the shallow groundwater table in the Ejina Delta generally does not exceed 6 m (Wang et al., 2014). However, in irrigated regions, the water table depth can surpass 10 m due to extensive groundwater extraction (Wang et al., 2011a). As indicated by Wang et al. (2014), groundwater dynamics are influenced by both natural hydrological processes (e.g., groundwater evapotranspiration and riverbank filtration) and human activities (e.g., groundwater pumping events and flood irrigation with surface water). The study by Wei et al. (2023) further indicates that the main influencing factors of the Ejina Delta shift from river water infiltration in the upper recharge

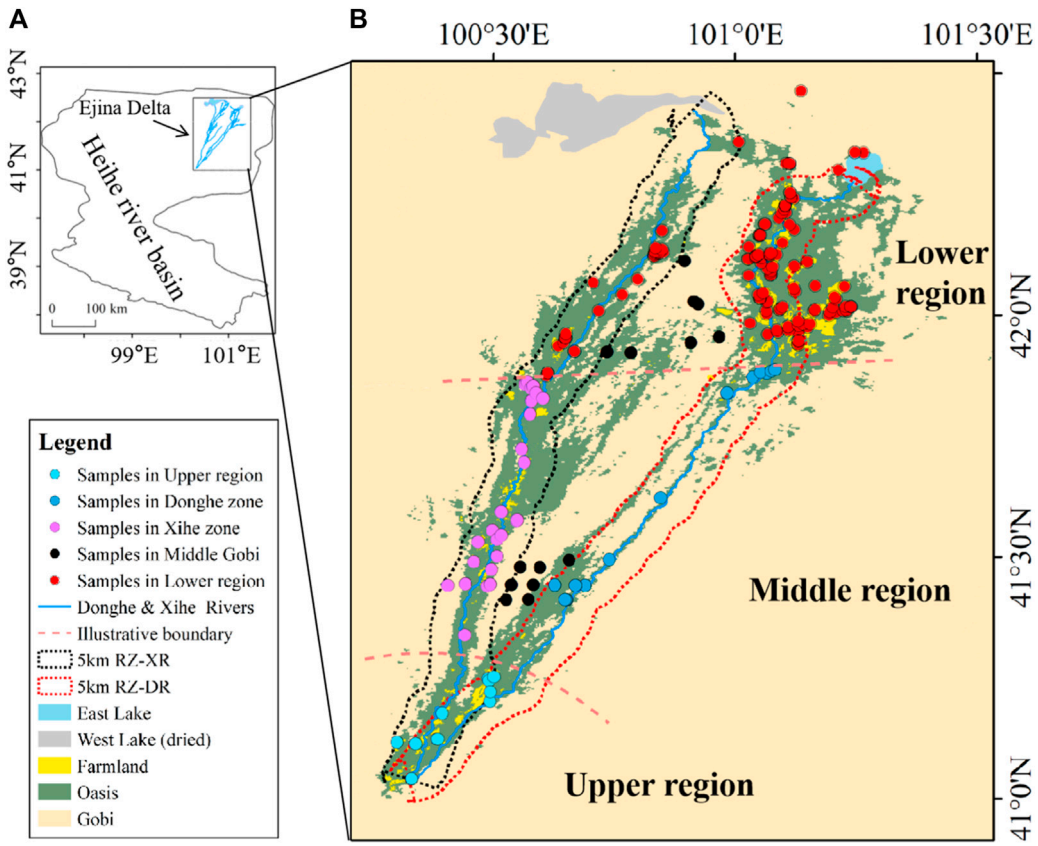

FIGURE 1
Map of the study area and distribution of sampling points. **(A)** Location of the Ejina Delta in the Heihe River basin, **(B)** Geographical map of the Ejina Delta. Orange dashed lines represent the indicative boundaries between the upper, middle, and lower regions of the Ejina Delta, 5 km RZ-XR and 5 km RZ-DR denote the 5 km range from the riverbank of Xihe and Donghe rivers, respectively.

area to cation exchange in the middle runoff area, and to groundwater evapotranspiration and leaching in the lower discharge area.

In this study, we analyzed 327 sets of groundwater samples collected from the lower Heihe River basin between 2001 and 2023. The objectives of this study are, therefore, as follows: 1) to detect the spatio-temporal changes in groundwater chemistry in the lower Heihe River basin, from upstream to downstream, as well as from riparian areas to the Gobi Desert; 2) to identify the predominant mechanisms that control the hydrochemical processes in arid river basins with intermittent river flows. This is of significant importance for maintaining sustainable development of regional groundwater, meeting the ecological balance and human needs in arid inland river basins (Hu et al., 2019; Wang et al., 2019).

2 Methods and materials

2.1 Study area

The Ejina Delta, on the northwestern Alxa Plateau, located in the lower reaches of the Heihe River in northwestern China (Figure 1), contends with an extremely arid climate, featuring a scanty average annual precipitation of approximately 35 mm (Wang et al., 2017) and a notably high average annual potential evapotranspiration of around 1,500 mm (Du et al., 2016; Liu et al., 2016). Over the period from 1961 to 2015, the mean annual air temperature in this area was about 9.1°C, with a maximum monthly mean air temperature of 27.1°C in July and a minimum of −11.2°C in January (Wang et al., 2017). However, the annual mean temperature from 1960 to 2017 in the Heihe River basin experienced statistically significant ($p < 0.05$) increases of 0.36 ± 0.09°C/decade based on the monitoring of meteorological stations (Peng et al., 2022).

Dominating the landscapes within the Ejina Delta is the Gobi region, characterized by wind-eroded hilly terrain, alkaline land, and desert (Wang et al., 2011a). Additionally, there are narrower strips of riparian vegetation along rivers, representing another, albeit less common, landform (Wang et al., 2011b). In recent years, the riparian vegetation coverage within the study area has significantly expanded, increasing from 1,619 km^2 in 2002–2,914 km^2 in 2020 (Zhang, 2023). The Ejina Delta is filled with unconsolidated Quaternary sediments, extending to a depth of several hundred meters (Wu et al., 2002). These sediments exhibit a gradual transition from coarse sand and gravel-pebble deposits to medium and fine sands from the southwest to the northeast within the study area (Wang et al., 2013; Yao et al., 2015; Vasilevskiy et al., 2022).

The Heihe River, originating from snowmelt and rainfall in the Qilian Mountains, bifurcates into two ephemeral streams, the Donghe and Xihe rivers, at the Langxinshan hydrological station. Subsequently, it flows through the Ejina Delta and reaches the East and West Juyan Lakes. The phreatic aquifer in the Ejina Delta is mainly recharged by Donghe and Xihe rivers, regulated by environmental flow controls (Wang et al., 2011a). In the latter half of the 20th century, excessive development and utilization in the middle and upper reaches of the Hei River led to a significant reduction in the flow duration of the lower Hei River (Ejina River), which directly caused a decline in groundwater levels and a decrease in groundwater volume in the Ejina Delta (Jiang and Liu, 2010). This resulted in a continuous deterioration of the ecological environment, manifested by oasis shrinkage, vegetation degradation, and an increase in the frequency of sandstorms (Zhang et al., 2011). To improve the local ecological environment, an *EWC* project, known as the Hei River "97" water diversion plan, was implemented from the year 2000, which involved intermittent artificial water transfer to the lower Hei River (Jiang et al., 2019). This *EWC* increased the river flow in the Ejina Delta, directing two-thirds of the surface runoff to the East River (Supplementary Figure S1) (Zhang J. et al., 2023). Additionally, the inflow from the Hei River is fresh water with a *TDS* concentration of about 300 mg/L (Kou et al., 2019). Its infiltration promotes groundwater recharge, helping to sustain groundwater resources and restore the groundwater ecosystem (Liu et al., 2022; Zhang J. et al., 2023). However, the extraction of groundwater with higher concentrations (*TDS* = 2,000 mg/L) for agricultural irrigation (Zhang et al., 2019) has led to two main issues: in some areas, the depth of the groundwater level exceeds 10 m, and it has also exacerbated the salinization of groundwater (Wang et al., 2011a).

In summary, the hydrogeological conditions in the Ejina Delta are notably intricate, characterized by uneven distribution of surface runoff and relatively concentrated agricultural irrigation in the lower region. As a result, significant spatiotemporal disparities exist in both water table depth (*WTD*) and hydrogeochemical characteristics of groundwater.

2.2 Data and methods

2.2.1 Sampling and data processing

The comprehensive water quality dataset spanning from 2001 to 2023 was compiled through meticulous literature review (Wang et al., 2011a; Qin et al., 2012) and field sampling. This dataset includes 327 groundwater samples collected from 192 locations (Figure 1), ensuring strict adherence to ion balance without outliers. These points, strategically placed in the riparian zones and desert regions of the Ejina Delta, include automatic monitoring wells for electrical conductivity (*EC*), water table depth (*WTD*), and water temperature (T_w) measurements, as well as local wells used for pastoral and irrigation (June, July and August) purposes. Before sampling, the well was pumped until water quality parameters such as pH, conductivity, and temperature have stabilized, at which point sampling can be conducted (Asubiojo et al., 1997). Water samples were collected in polyethylene bottles, sealed with parafilm, and stored at 4°C before testing within 1 week of collection (Liu et al., 2023).

Parameters measured in the field included major ion concentrations, *pH*, *EC*, *WTD*, *and* T_w, using a portable conductivity meter (HI98188, HANNA) and a handheld meter (CyberScan PC300) for *pH*, *EC*, T_w, and Oxidation-Reduction Potential (ORP). Total dissolved solids (*TDS*) concentrations were computed by summing the concentrations of major ions, which include cations (Na^+, K^+, Ca^{2+} and Mg^{2+}) and anions (Cl^-, SO_4^{2-} and HCO_3^-). *WTD* data were recorded for selected monitoring wells. Groundwater samples were analyzed for cations using an inductively coupled plasma spectrometer (iCAP-7400, Thermo Fisher, United States) and for anions using an ion chromatograph (ICS2100, Thermo Fisher, United States) (Zhang et al., 2021). HCO_3^- quantification involved titration with a 0.01 mol/L sulfuric acid solution (Zhang et al., 2021). Before analysis, groundwater samples were filtered through 0.45 μm filter membranes and diluted to an *EC* of <1 mS/cm to prevent potential instrument damage.

2.2.2 Analytical methods

The hydrogeochemical simulations were executed using the PHREEQC software (Parkhurst and Appelo, 2013), with an established uncertainty threshold set at 0.1. For the inverse modeling, the "phreeqc.dat" database (Parkhurst and Appelo, 1999) was chosen to provide the thermodynamic data. In the examination of water-rock interactions, the mineral saturation index (*SI*) was used in order to describe the state of minerals in relation to their solubility in water. Subsequently, quantities of dissolution, precipitation, and migration-transformation of minerals were determined through reverse geochemical simulations. The formula for *SI* is expressed as follows (Zhang et al., 2021):

$$SI = \log_{10}(IAP/K) \quad (1)$$

where *IAP* represents the ion activity product, and *K* denotes the reaction equilibrium constant.

During the process of hydrogeochemical simulations, this study further delineated regions and selected hydrogeochemical simulation paths based on the locations of sampling points. The Ejina Delta were divided into upper, middle, and lower regions along the direction of water flow, and laterally into riparian zone (within 5 km of the main river channel) and Middle Gobi zone (Figure 2). In the investigation of groundwater water-rock interactions, 81 sample data points from 13 long-term automatic monitoring wells in various zones were selected for analysis. 8 interaction paths (U-X, U-M, U-D, X-L, M-LM-1, M-LM-2, D-LM, LM-L in Figure 2) were established along the direction of water flow, comprehensively covering the Ejina Delta region.

3 Results

3.1 Spatial variation of hydrochemical variables

The multiyear mean *TDS* concentration of the groundwater in the Ejina Delta was approximately 1,527.4 ± 1,059.5 mg/L from 2001 to 2023, revealing substantial spatial variations among different

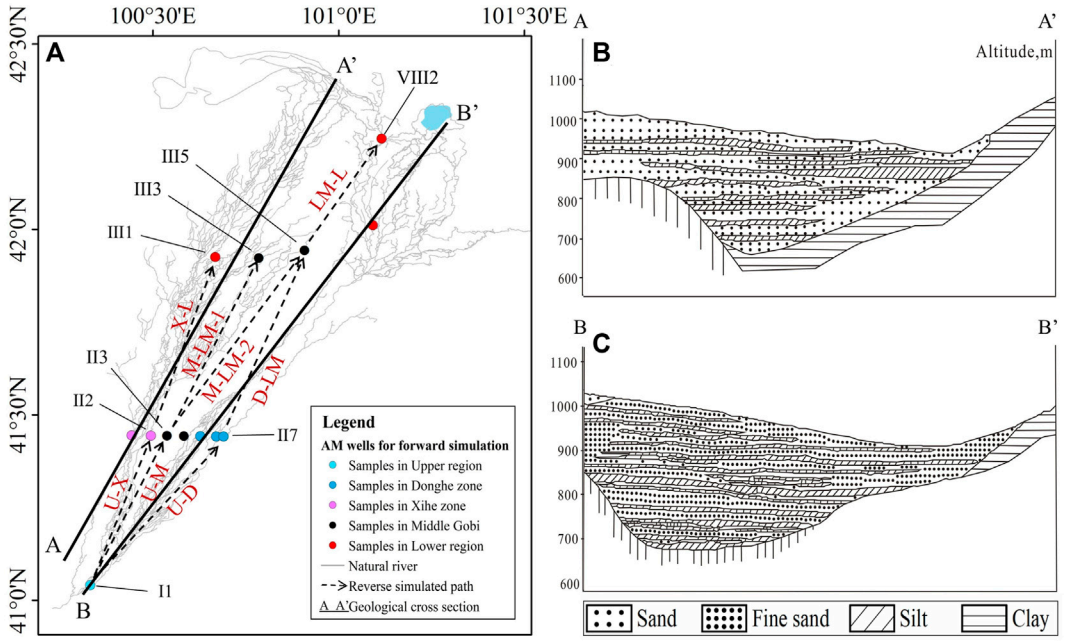

FIGURE 2
(A) schematic diagram of water-rock interaction analysis paths. AM wells stands for automatic monitoring well. **(B, C)** are the geological profiles, which is modified from (Xi et al., 2010a; Wang et al., 2014).

zones (Table 1). In the upper region, characterized by a relatively uniform lithological structure and coarse-grained aquifers, groundwater *TDS* concentrations are relatively low (881.5 ± 331.6 mg/L), dominated by Na-Mg-SO_4-HCO_3 and Na-Mg-Ca-SO_4-HCO_3 hydrochemical types (Figure 3). Along with the flow paths, the aquifer permeability gradually decreases, yet the Donghe and Xihe riparian zones maintain comparatively low groundwater *TDS* concentrations (900.8 ± 469.9 mg/L and 1,077.6 ± 541.0 mg/L, respectively), governed mainly by the Na-Mg-SO_4-HCO_3 water chemistry type. However, in the Middle Gobi, groundwater *TDS* concentrations are approximately 1,143.2 ± 585.7 mg/L, with a significant shift in the dominant water chemistry type occurs, transitioning to Na-SO_4-Cl. In the lower region, characterized by the highest *TDS* concentrations (1,953.6 ± 1,208.5 mg/L), the primary water chemistry types are Na-Mg-SO_4-HCO_3 and Na-Mg-SO_4-Cl.

The groundwater *TDS* concentration in the upper region is relatively stable and low with values ranging from 0.61×10^3 to 1.20×10^3 mg/L and no apparent inter-annual trend (Figure 4). In the middle region, the groundwater *TDS* concentration is overall higher than that of the upper region, ranging from 0.57×10^3 to 1.71×10^3 mg/L, indicating a higher degree of mineralization (Figure 4). At the same time, the *TDS* concentration in the Middle Gobi is higher than that of the riparian zone, with no significant overall inter-annual trend. The lower region has the highest and most variable groundwater *TDS* concentrations, indicating the highest degree of mineralization at the downstream delta (Figure 4). Although the groundwater *TDS* concentration in the lower region fluctuates in different years, there is an overall upward trend, with concentrations ranging from 1.33×10^3 to 2.94×10^3 mg/L (Figure 4). Additionally, the data from 2017, 2021, and 2023 show a declining trend in recent years (Figure 4). However, it is noteworthy that the sampling in 2023 was carried out in mid-March, coinciding with the *EWC* from the middle and upper reaches to the lower reaches, which may result in a generally lower TDS concentration in the groundwater across the entire study area.

The multiyear average *WTD* in the Ejina Delta from 2001 to 2021 was around 3.8 ± 2.2 m, ranging from 0.7 to 12.7 m (Table 1). Significant spatial variations in *WTD* were evident across Ejina Delta, with the lowest *WTD* of 2.4 ± 0.6 m in the Xihe zone and the highest *WTD* of 4.6 ± 2.7 m in the lower region. The Donghe zone, with an average *WTD* of 2.9 ± 0.9 m, was followed by the upper region at 3.2 ± 0.8 m, and the Middle Gobi at 3.4 ± 1.0 m. The lower region exhibited the most pronounced fluctuations in *WTD* (SD = 2.7), while other zones showed minor fluctuations over the years, with SD less than or equal to 1.0 m. The multiyear annual T_w of the Ejina Delta during the period of 2009–2023 was 13.0°C ± 3.9°C, varying from 0.7°C to 22.6°C across all these zones. The multiyear annual T_w in the upper region was the lowest (11.0°C ± 3.4°C), while the Xihe zone had the highest multiyear annual T_w (14.7°C ± 4.3°C).

The groundwater within the Ejina Delta consistently exhibited a slightly alkaline nature, as evidenced by a stable multiyear annual *pH* of 7.8 ± 0.4 (Table 1). Zonal heterogeneity emerged in the major ion composition (Na^+, K^+, Mg^{2+}, Ca^{2+}, SO_4^{2-}, Cl^- and HCO_3^-) across the Ejina Delta from 2001 to 2023. The major ion concentration of groundwater showed a persistent spatial variation with *TDS* concentrations, ion concentrations in the lower region approximately 2–3 times higher than those in the upper region. Furthermore, the middle region, including the Donghe zone, Xihe zone and Middle Gobi, had significantly lower multiyear annual

10.3389/fenvs.2024.1376443

TABLE 1 Hydrochemical characteristics of the groundwater in the Ejina Delta and different zones (2001–2023).

Parameters	Ejina delta				Donghe zone				Xihe zone			
	Max.	Min.	Mean	SD	Max.	Min.	Mean	SD	Max.	Min.	Mean	SD
WTD(m)	12.7	0.7	3.8	2.2	5.0	1.8	2.9	0.9	4.0	1.5	2.4	0.6
T_w(°C)	22.6	0.7	13.0	3.9	19.3	3.6	13.0	4.3	21.5	3.8	14.7	4.3
ORP(mV)	352.0	−165.0	138.0	107.8	286.0	−94.6	149.9	133.6	259.0	−4.8	163.2	75.4
EC(ms/cm)	21.6	0.6	2.8	2.4	5.9	0.6	1.8	1.1	4.3	0.7	2.0	1.0
pH	9.8	6.5	7.8	0.4	8.7	7.0	7.8	0.4	8.8	7.4	7.8	0.3
TDS(mg/L)	5,793.5	454.6	1,527.4	1,059.5	2,982.5	454.6	900.8	469.9	2,754.9	569.2	1,077.6	541.0
Na^+(mg/L)	1,617.6	47.0	289.7	222.3	782.7	47.0	181.0	146.0	632.0	89.5	225.1	140.5
K^+(mg/L)	233.6	1.0	12.5	16.2	35.0	4.0	9.9	5.5	36.0	4.9	11.0	5.9
Mg^{2+}(mg/L)	483.3	8.0	107.2	90.6	121.5	14.2	56.2	25.2	223.0	27.5	66.0	33.3
Ca^{2+}(mg/L)	328.8	4.9	89.2	56.5	123.5	12.4	56.2	23.0	104.9	12.4	54.8	19.0
SO_4^{2-}(mg/L)	2,760.0	51.4	592.1	493.8	1,390.0	51.4	315.8	239.8	1,328.0	73.8	392.5	246.8
Cl^-(mg/L)	2,155.1	38.7	269.2	249.7	421.2	45.6	144.2	84.2	558.1	54.3	181.6	119.2
HCO_3^-(mg/L)	1,299.3	90.3	340.5	176.0	527.7	151.0	279.6	65.0	1,033.0	91.5	297.8	132.7
Parameters	Upper region				Middle Gobi				Lower region			
	Max.	Min.	Mean	SD	Max.	Min.	Mean	SD	Max.	Min.	Mean	SD
WTD(m)	4.9	2.2	3.2	0.8	6.2	2.0	3.4	1.0	12.7	0.7	4.6	2.7
T_w(°C)	17.0	5.6	11.0	3.4	18.1	3.0	12.7	3.5	22.6	0.7	12.8	3.8
ORP(mV)	352.0	89.5	215.6	98.1	274.0	−67.2	142.2	128.5	242.0	−165.0	122.2	102.4
EC(ms/cm)	3.4	0.9	1.5	0.7	6.3	0.8	2.2	1.3	21.6	0.7	3.6	2.9
pH	8.5	7.3	7.7	0.3	8.9	7.2	7.8	0.4	9.8	6.5	7.8	0.5
TDS(mg/L)	1825.3	606.8	881.5	331.6	2,688.3	551.2	1,143.2	585.7	5,793.5	536.2	1953.6	1,208.5
Na^+(mg/L)	343.3	83.1	124.4	57.7	628.2	113.9	260.2	131.5	1,617.6	69.8	356.2	257.5
K^+(mg/L)	20.0	5.7	7.7	3.3	17.4	1.5	11.7	3.5	233.6	1.0	14.3	21.5
Mg^{2+}(mg/L)	143.0	51.3	76.5	29.0	128.1	11.6	56.3	28.4	483.3	8.0	146.0	106.0
Ca^{2+}(mg/L)	127.3	52.4	71.8	21.4	150.6	13.1	58.8	33.6	328.8	4.9	115.3	62.2
SO_4^{2-}(mg/L)	791.3	59.2	319.0	176.5	1,211.0	73.2	424.4	285.6	2,760.0	52.7	778.5	569.1
Cl^-(mg/L)	262.0	59.7	139.9	63.5	1,067.5	67.1	212.3	167.1	2,155.1	38.7	348.2	297.8
HCO_3^-(mg/L)	535.0	221.7	289.3	69.9	552.8	90.3	243.2	81.3	1,299.3	109.8	397.0	206.3

Note: SD represents standard deviations.

concentrations of Mg^{2+}, Ca^{2+} and HCO_3^-, which were 59.5 ± 29.0 mg/L, 56.6 ± 25.2 mg/L, 273.5 ± 93.0 mg/L, respectively.

In the entire area, Na^+ exhibited the highest cation concentration (289.7 ± 222.3 mg/L), while SO_4^{2-} showed a relatively higher anion concentration (592.1 ± 493.8 mg/L). However, noteworthy differences in ion proportions were observed among the different zones. Cl^- and HCO_3^- had similar proportions in the Ejina Delta, representing 28.4 ± 11.7 meq% and 25.9 ± 9.7 meq%, respectively. In the upper region, Mg^{2+} had the highest proportion among cations, accounting for 40.5 ± 3.9 meq% (Table 1). In the Middle Gobi and lower region, characterized by less river water recharge, the proportion of Cl^- was higher than HCO_3^-, while in well-recharged zones such as the upper region and the riparian zones, HCO_3^- was dominant than Cl^-, which aligned with the prevalent hydrochemical types of groundwater in these zones.

According to Supplementary Figure S2F, SO_4^{2-} is the ion with the most significant interannual variation in the groundwater of the Ejina Delta, followed by Cl^- and Na^+. Furthermore, the variation trend of SO_4^{2-} aligns closely with that of *TDS*, indicating that the dissolution of sulfate minerals plays a significant role in shaping the

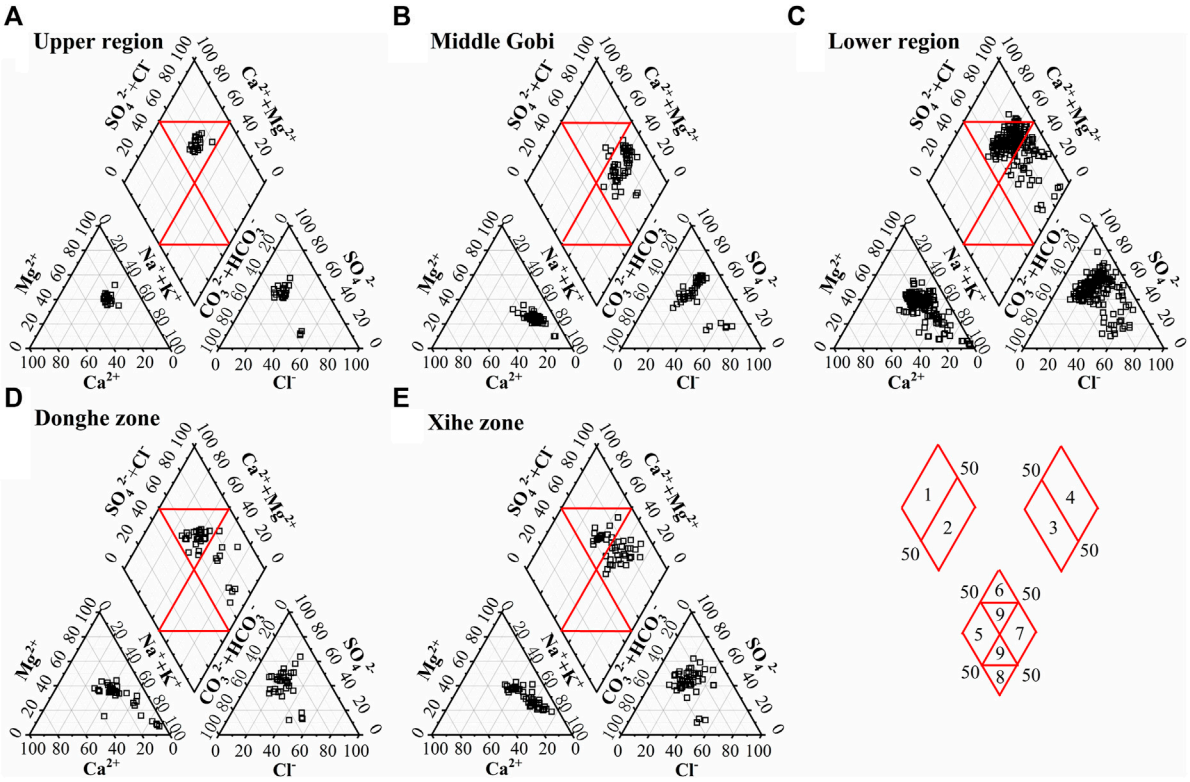

FIGURE 3
Piper diagrams (Piper, 1944) depicting groundwater chemistry in the Ejina Delta (2001–2023) with hydrochemical type distinctions (the red line in the bottom right). **(A–E)** represent Piper diagrams for the upper region, Middle Gobi, lower region, Donghe zone, and Xihe zone, respectively. 1-Alkaline earths (Ca^{2+} + Mg^{2+}) exceed alkalis (Na^{+} + K^{+}); 2-Alkalis exceed alkaline earths; 3-Weak acids (CO_3^{2-} + HCO_3^{-}) exceed strong acids (SO_4^{2-} + Cl^{-}); 4-Strong acids exceed weak acids; 5-Carbonate hardness >50% (alkaline earths and weak acid dominate); 6-Non-carbonate hardness >50%; 7-Non-carbonate alkali >50%; 8-Carbonate alkali >50; 9-No cation-anion pair >50%.

chemical characteristics of groundwater across different regions (Jiang et al., 2022). Apart from HCO_3^{-}, Cl^{-} and Na^{+}, the other ions generally experienced two peaks in 2011 and 2017, with the highest values occurring in 2017. From 2001 to 2023, the concentrations of major ions in the upper region and riparian zones were lower, generally below 500 mg/L, and showed a declining trend in both the upper region and the Xihe River (Supplementary Figure S2). The concentrations of major ions in the lower region were higher and exhibited an increasing trend.

In the groundwater chemistry dataset of this study, the number of data from monitoring wells is 106, whereas the number of data from irrigation wells stands at 221, which is more than double the number of the monitoring wells (Supplementary Table S1). Focusing on the water chemical components, the average concentration of *TDS* in irrigation wells is 1,742.0 mg/L, significantly higher than that in monitoring wells, which is 1,080.1 mg/L. This indicates that irrigation promotes the evaporation-crystallization processes of groundwater. Similarly, the concentrations of Na^{+}, Mg^{2+}, Ca^{2+}, SO_4^{2-}, Cl^{-}, and HCO_3^{-} in groundwater from irrigation wells are generally higher than those from monitoring wells (Supplementary Table S1). Notably, the concentrations of Mg^{2+} and SO_4^{2-} in groundwater from irrigation wells are almost double those from monitoring wells. Moreover, high concentrations of sodium and chloride may indicate the impact of salinization in the area of the irrigation wells, which is a common issue in the process of irrigation water use, as irrigation can lead to the accumulation of salts in the soil with the rising of groundwater level.

3.2 Temporal variation of hydrochemical variables

3.2.1 Interannual variation of hydrochemical variables

The temporal variation of *TDS* in the groundwater of Ejina Delta exhibits a complex pattern, characterized by intricate fluctuations over the past 23 years (Supplementary Table S2). The *TDS* concentrations in the upper region declined from 1,200.6 mg/L in 2001 to approximately 600–800 mg/L after 2009, with an exception in 2011 (*TDS* reached 1,012.2 mg/L). The Xihe zone displayed a more pronounced decrease in *TDS* concentration, dropping from 1,347.3 mg/L in 2001 to 808.0 mg/L in 2023. Conversely, *TDS* variations in the Donghe zone, Middle Gobi, and lower region were intricate, featuring notably higher *TDS* concentrations during 2011–2017. For instance, the lower region exhibited a mean annual *TDS* of 1,953.6 mg/L, rising to a peak of 2,938.9 mg/L in 2017, followed by a decline to 1,333.9 mg/L in 2023 (Supplementary Table S2). From 2001 to 2023, the predominant groundwater chemistry in the Ejina Delta comprised Na-Mg-SO_4-HCO_3, Na-Mg-SO_4-Cl and Na-SO_4-Cl. However, noteworthy deviations were observed in

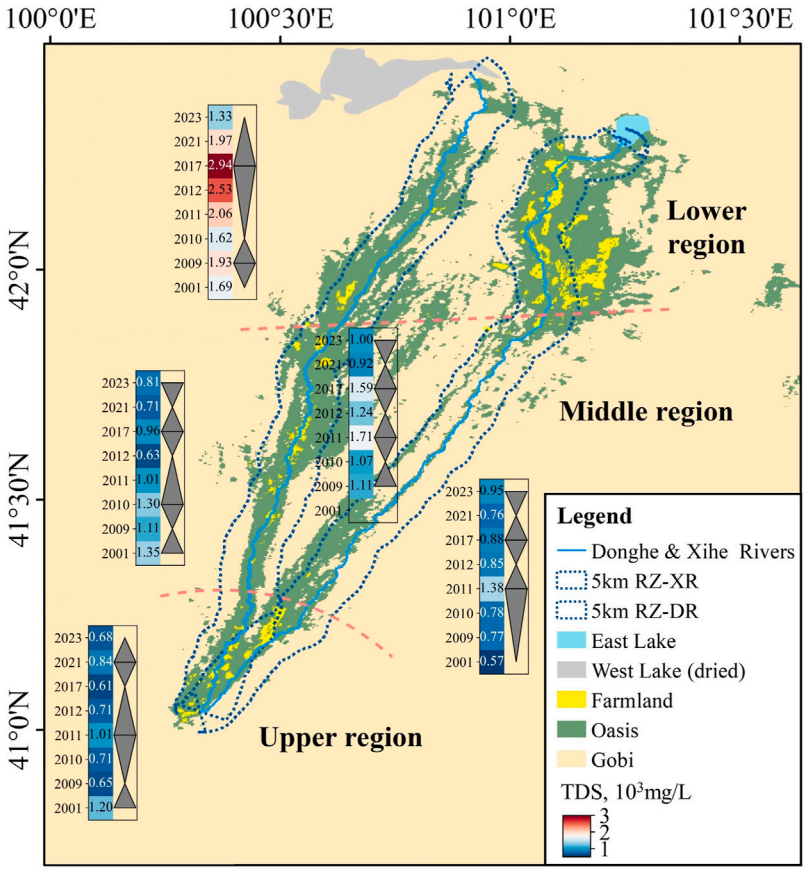

FIGURE 4
Map of regional spatial changes in *TDS* concentration from 2001 to 2023. The inverted triangle and triangle represent increasing and decreasing trend of *TDS* concentration, respectively.

2009 and 2011, with Na-Mg-HCO_3-Cl and Na-Mg-SO_4-Cl emerging as the primary water chemistry types, respectively.

The upper region generally shows lower *TDS* concentrations (Supplementary Figure S3). Additionally the *TDS* concentration in the middle region does not vary significantly, while in the lower region exhibiting the greatest changes. Notably, during the year of 2017, *TDS* concentration of groundwater in the lower region was very high (2.94×10^3 mg/L) (Figure 3) with a following decreasing trend in 2023 (Supplementary Figure S3). Overall, the groundwater *TDS* concentrations in 2010 and 2023 were lower.

Over the past 23 years, the overall groundwater table in the Ejina Delta has exhibited fluctuations within a range of about 4 m, with the riparian zones significantly higher than other areas. Notably, the mean annual *WTD* in Donghe zone demonstrates a distinct rebound, recovering from ~ 4 m in 2001 to over 2.5 m after 2012, while other regions show no significant trend.

Throughout the entirety of the Ejina Delta, the *pH* values, groundwater temperature and concentrations of major ions exhibited no significant changes over the 23-year study period. However, Consistent with the temporal trends of *TDS*, concentrations of Na^+ and Cl^- displayed notable decreases in the upper region and Xihe zone. For instance, the Cl^- concentration decreased from 267.7 mg/L in 2001 to around 80 mg/L in recent years. It is noteworthy that, despite a consistent decrease in SO_4^{2-} concentrations in the Xihe zone, there was a discernible relative increase in the Donghe zone, rising from around 170 mg/L before 2009 to 361.3 mg/L in 2023 (Supplementary Table S2).

3.2.2 Seasonal variation of hydrochemical variables

Seasonal differences in hydrochemical characteristics were observed in the Ejina Delta across different zones from 2001 to 2023 (Table 2). The annual hydrological cycle exhibited distinctive patterns in groundwater *TDS* concentrations. Higher values were observed during summer (1,589.4 ± 1,128.5 mg/L) and autumn (1,506.3 ± 853.0 mg/L), while the lowest values occurred in spring (1,120.4 ± 708.7 mg/L) (Table 2). Spatial variations were significant, with the upper region and Xihe zone displaying similar seasonal features, while the Middle Gobi, lower region, and Donghe zone exhibited different and more complex seasonal patterns.

The groundwater *TDS* concentration in the Ejina Delta is relatively lower in spring and significantly higher in summer, demonstrating a distinct seasonal pattern (Figure 5). The spatial distribution of groundwater *TDS* shows a gradient from the upper to lower regions in all seasons, with the lowest concentrations in the upper region, and the highest in the lower region. This is likely due to evaporation crystallization, agricultural irrigation, and reduced ecological water transfer replenishment, which may lead to the enrichment of minerals in the groundwater of the lower region.

TABLE 2 Seasonal hydrochemical variations in groundwater across the Ejina Delta (2001–2023).

		WTD	T_w	*ORP*	*EC*	*pH*	*TDS*	Na	K	Mg	Ca	SO_4	Cl	HCO_3
		m	˚C	mV	ms/cm		mg/L	mg/L	mg/L	mg/L	mg/L	mg/L	mg/L	mg/L
Ejina Delta	Spring	2.7 ± 1.2 (*n* = 12)	8.7 ± 3.8 (*n* = 34)	130.9 ± 143.4 (*n* = 34)	1.7 ± 0.9 (*n* = 34)	7.5 ± 0.3 (*n* = 13)	1,120.4 ± 708.7 (*n* = 34)	213.5 ± 152.4 (*n* = 34)	11.0 ± 5.6 (*n* = 34)	76.1 ± 58.8 (*n* = 34)	70.0 ± 38.4 (*n* = 34)	457.2 ± 360.5 (*n* = 34)	152.1 ± 94.2 (*n* = 34)	285.5 ± 105.0 (*n* = 34)
	Summer	3.7 ± 2.3 (*n* = 119)	13.7 ± 3.5 (*n* = 213)	141.0 ± 89.4 (*n* = 80)	3.0 ± 2.5 (*n* = 219)	7.7 ± 0.4 (*n* = 219)	1,589.4 ± 1,128.5 (*n* = 241)	310.4 ± 242.1 (*n* = 241)	13.1 ± 18.5 (*n* = 241)	110.9 ± 94.7 (*n* = 241)	90.9 ± 57.9 (*n* = 241)	611.8 ± 524.2 (*n* = 241)	287.8 ± 274.5 (*n* = 241)	334.4 ± 175.1 (*n* = 241)
	Autumn	4.3 ± 2.0 (*n* = 47)	12.9 ± 0.8 (*n* = 4)		2.1 ± 0.6 (*n* = 5)	8.0 ± 0.3 (*n* = 49)	1,506.3 ± 853.0 (*n* = 52)	243.7 ± 130.0 (*n* = 52)	10.6 ± 5.6 (*n* = 52)	110.5 ± 85.3 (*n* = 52)	93.7 ± 57.9 (*n* = 52)	589.2 ± 408.9 (*n* = 52)	259.6 ± 165.7 (*n* = 52)	404.7 ± 200.4 (*n* = 52)
Upper region	Spring		8.5 ± 4.1 (*n* = 2)	233.0 ± 168.3 (*n* = 2)	1.1 ± 0.2 (*n* = 2)	7.3± (*n* = 1)	692.9 ± 17.5 (*n* = 2)	89.2 ± 0.7 (*n* = 2)	6.4 ± 0.9 (*n* = 2)	60.8 ± 0.6 (*n* = 2)	65.3 ± 2.4 (*n* = 2)	281.3 ± 1.7 (*n* = 2)	79.4 ± 16.5 (*n* = 2)	224.5 ± 3.9 (*n* = 2)
	Summer	3.3 ± 0.9 (*n* = 7)	11.5 ± 3.3 (*n* = 12)	206.8 ± 79.3 (*n* = 4)	1.6 ± 0.7 (*n* = 12)	7.7 ± 0.2 (*n* = 12)	794.6 ± 313.1 (*n* = 14)	120.2 ± 67.3 (*n* = 14)	7.3 ± 3.7 (*n* = 14)	66.7 ± 23.2 (*n* = 14)	69.1 ± 20.9 (*n* = 14)	264.8 ± 176.5 (*n* = 14)	133.4 ± 64.5 (*n* = 14)	269.5 ± 30.7 (*n* = 14)
	Autumn	3.0 ± 0.6 (*n* = 5)				8.0 ± 0.3 (*n* = 5)	1,200.6 ± 244.0 (*n* = 5)	148.2 ± 23.1 (*n* = 5)	9.4 ± 2.1 (*n* = 5)	110.0 ± 24.5 (*n* = 5)	81.8 ± 26.4 (*n* = 5)	485.8 ± 93.1 (*n* = 5)	182.6 ± 47.6 (*n* = 5)	370.8 ± 97.9 (*n* = 5)
Middle Gobi	Spring	3.3 ± 0.5 (*n* = 4)	9.3 ± 3.7 (*n* = 12)	149.3 ± 134.9 (*n* = 12)	1.8 ± 0.9 (*n* = 12)	7.6 ± 0.3 (*n* = 4)	1,119.4 ± 604.0 (*n* = 12)	254.2 ± 138.0 (*n* = 12)	11.9 ± 2.2 (*n* = 12)	54.9 ± 27.2 (*n* = 12)	56.1 ± 32.9 (*n* = 12)	457.8 ± 294.8 (*n* = 12)	175.4 ± 95.6 (*n* = 12)	221.6 ± 46.7 (*n* = 12)
	Summer	3.4 ± 1.2 (*n* = 14)	14.6 ± 2.0 (*n* = 23)	113.8 ± 118.5 (*n* = 3)	2.4 ± 1.5 (*n* = 23)	7.8 ± 0.4 (*n* = 23)	1,154.7 ± 614.1 (*n* = 33)	265.2 ± 136.8 (*n* = 33)	11.4 ± 3.9 (*n* = 33)	57.8 ± 30.5 (*n* = 33)	60.2 ± 35.6 (*n* = 33)	417.2 ± 299.3 (*n* = 33)	231.6 ± 192.9 (*n* = 33)	226.5 ± 55.0 (*n* = 33)
	Autumn	3.7 ± 0.2 (*n* = 3)	12.6 ± 0.7 (*n* = 3)		2.1 ± 0.7 (*n* = 3)	7.6 ± 0.2 (*n* = 3)	1,120.2 ± 352.5 (*n* = 4)	235.2 ± 77.3 (*n* = 4)	13.5 ± 3.3 (*n* = 4)	49.1 ± 15.1 (*n* = 4)	55.1 ± 23.6 (*n* = 4)	384.3 ± 156.2 (*n* = 4)	163.3 ± 59.5 (*n* = 4)	446.0 ± 75.7 (*n* = 4)
Lower region	Spring	3.1 ± 2.4 (*n* = 3)	8.5 ± 4.5 (*n* = 8)	79.7 ± 147.4 (*n* = 8)	2.3 ± 1.1 (*n* = 8)	7.3 ± 0.2 (*n* = 3)	1,668.2 ± 1,088.7 (*n* = 8)	267.7 ± 234.8 (*n* = 8)	13.6 ± 8.9 (*n* = 8)	142.3 ± 88.3 (*n* = 8)	112.6 ± 43.9 (*n* = 8)	738.1 ± 568.1 (*n* = 8)	200.9 ± 130.0 (*n* = 8)	392.4 ± 133.6 (*n* = 8)
	Summer	4.4 ± 2.8 (*n* = 63)	13.1 ± 3.6 (*n* = 128)	128.1 ± 94.8 (*n* = 58)	3.6 ± 2.9 (*n* = 133)	7.7 ± 0.5 (*n* = 133)	2020.2 ± 1,266.6 (*n* = 136)	381.1 ± 276.2 (*n* = 136)	15.5 ± 24.1 (*n* = 136)	149.9 ± 109.1 (*n* = 136)	116.1 ± 62.7 (*n* = 136)	796.4 ± 592.8 (*n* = 136)	367.6 ± 323.9 (*n* = 136)	393.8 ± 208.6 (*n* = 136)
	Autumn	5.1 ± 2.2 (*n* = 28)			2.5± (*n* = 1)	8.1 ± 0.3 (*n* = 31)	1742.2 ± 950.5 (*n* = 32)	272.7 ± 132.5 (*n* = 32)	9.3 ± 4.7 (*n* = 32)	130.3 ± 97.5 (*n* = 32)	112.3 ± 65.3 (*n* = 32)	712.5 ± 467.8 (*n* = 32)	302.5 ± 174.7 (*n* = 32)	411.8 ± 215.5 (*n* = 32)
Donghe zone	Spring	2.4 ± 0.4 (*n* = 3)	7.5 ± 2.6 (*n* = 7)	123.6 ± 175.8 (*n* = 7)	1.4 ± 0.2 (*n* = 7)	7.6 ± 0.3 (*n* = 3)	891.2 ± 213.0 (*n* = 7)	168.5 ± 85.0 (*n* = 7)	8.7 ± 1.9 (*n* = 7)	61.6 ± 26.1 (*n* = 7)	58.3 ± 21.4 (*n* = 7)	327.6 ± 91.6 (*n* = 7)	126.7 ± 38.2 (*n* = 7)	284.3 ± 55.7 (*n* = 7)
	Summer	2.9 ± 0.9 (*n* = 17)	14.9 ± 2.9 (*n* = 20)	180.6 ± 60.7 (*n* = 6)	1.9 ± 1.3 (*n* = 20)	7.8 ± 0.4 (*n* = 20)	942.7 ± 544.6 (*n* = 24)	198.7 ± 166.9 (*n* = 24)	10.5 ± 6.3 (*n* = 24)	57.2 ± 25.7 (*n* = 24)	54.4 ± 23.7 (*n* = 24)	331.3 ± 282.3 (*n* = 24)	157.5 ± 96.0 (*n* = 24)	270.6 ± 50.8 (*n* = 24)
	Autumn	3.6 ± 1.0 (*n* = 4)	13.7± (*n* = 1)		1.9± (*n* = 1)	8.0 ± 0.1 (*n* = 3)	666.1 ± 222.3 (*n* = 4)	96.7 ± 36.9 (*n* = 4)	8.2 ± 3.4 (*n* = 4)	40.7 ± 19.9 (*n* = 4)	63.2 ± 25.5 (*n* = 4)	202.4 ± 65.5 (*n* = 4)	94.9 ± 36.9 (*n* = 4)	325.4 ± 137.7 (*n* = 4)
Xihe zone	Spring	1.6 ± 0.1 (*n* = 2)	9.2 ± 4.9 (*n* = 5)	138.1 ± 128.5 (*n* = 5)	1.2 ± 0.3 (*n* = 5)	7.8 ± 0.1 (*n* = 2)	738.3 ± 180.7 (*n* = 5)	141.6 ± 57.4 (*n* = 5)	9.9 ± 7.9 (*n* = 5)	47.6 ± 13.3 (*n* = 5)	53.4 ± 17.7 (*n* = 5)	258.3 ± 61.9 (*n* = 5)	82.8 ± 9.0 (*n* = 5)	293.9 ± 109.2 (*n* = 5)

(Continued on following page)

10.3389/fenvs.2024.1376443

TABLE 2 (*Continued*) Seasonal hydrochemical variations in groundwater across the Ejina Delta (2001–2023).

		WTD	T_w	*ORP*	*EC*	*pH*	*TDS*	Na	K	Mg	Ca	SO_4	Cl	HCO_3
		m	°C	mV	ms/cm		mg/L	mg/L	mg/L	mg/L	mg/L	mg/L	mg/L	mg/L
	Summer	2.5 ± 0.6 (n = 18)	15.6 ± 3.5 (n = 30)	177.1 ± 19.3 (n = 9)	2.1 ± 1.0 (n = 31)	7.8 ± 0.3 (n = 31)	1,072.0 ± 535.2 (n = 34)	228.6 ± 145.3 (n = 34)	9.9 ± 4.2 (n = 34)	62.8 ± 23.6 (n = 34)	54.7 ± 20.6 (n = 34)	403.0 ± 273.2 (n = 34)	178.4 ± 102.0 (n = 34)	273.7 ± 71.4 (n = 34)
	Autumn	2.3 ± 0.6 (n = 7)				8.1 ± 0.3 (n = 7)	1,347.3 ± 645.8 (n = 7)	267.9 ± 147.4 (n = 7)	17.0 ± 8.7 (n = 7)	95.0 ± 61.9 (n = 7)	56.4 ± 12.8 (n = 7)	437.7 ± 160.4 (n = 7)	267.7 ± 180.3 (n = 7)	418.0 ± 275.4 (n = 7)

Note: 1) Data are presented as mean ± one standard deviation; 2) "n" represents the amount of groundwater samples; 3) *TDS* and major ion concentrations were derived from 327 non-continuous groundwater samples collected in 2001, 2009, 2010, 2011, 2012, 2017, 2021 and 2023; 4) *WTD*, T_w, *ORP*, *EC* and *pH* from the 327 sets of groundwater samples were incomplete due to sampling conditions; 5) Seasonal classification: Spring (March to May), summer (June to August), autumn (September to November), and winter (December to the following February).

In spring, the *TDS* concentrations in the upper region are the lowest among the three regions (Figure 5A). The middle region shows moderate *TDS* levels, and the lower region starts to show increased concentrations, although not as high as in other seasons. The overall distribution of *TDS* is relatively uniform, with a gradual increase from the upper to the lower region. In summer, the map shows more significant variation in *TDS* concentrations. There is a notable increase in *TDS* levels in the lower region, suggesting a higher degree of mineralization (Figure 5B). This could be attributed to reduced dilution and increased mineral dissolution due to decreased river flows, groundwater extraction for irrigation, and higher evaporation rates during the warmer months. The sampling mainly took place in the summer, and the number of irrigation wells significantly exceeds that of monitoring wells. Additionally, monitoring wells are relatively closer to the rivers, which further explains the lower groundwater *TDS* concentrations observed in the monitoring wells mentioned earlier. In autumn, the *TDS* concentrations in the lower region seem to decrease slightly compared to summer, possibly due to the end of the growing season and reduced irrigation (Figure 5C). The *TDS* concentrations in the upper and middle regions remain fairly consistent with spring levels, maintaining a moderate level of mineralization.

In the Ejina Delta, the hydrogeochemical composition consistently featured Na-Mg-SO_4-HCO_3 predominance throughout all seasons. Notably, during the summer and autumn seasons, Na-Mg-SO_4-Cl groundwater was also present, constituting 15.8% and 19.2%, respectively. Na^+ dominated with milliequivalent percentages of 47.8%, 48.4%, 44.1% during spring, summer, and autumn, respectively. Simultaneously, SO_4^{2-} maintained its role as the primary anion, comprising milliequivalent percentage of 48.6%, 45.5%, 44.6% during these three seasons, respectively. Additionally, Cl^- and HCO_3^- exhibited comparable milliequivalent percentages around 22.5%–42.9% and 22.5%–31.1%, with slightly fluctuations across different years.

The *WTD* and T_w in the Ejina Delta exhibit pronounced seasonal characteristics. In general, T_w reached its lowest point in spring (8.7°C ± 3.8°C) and peaks in summer (13.7°C ± 3.5°C). On the other hand, *WTD* values are at their maximum in autumn (4.3 ± 2.0 m) and minimum in spring (2.7 ± 1.2 m). Notably, in the upper region and Xihe zone, summer is the season with the highest *WTD* values, reaching 3.3 ± 0.9 m and 2.5 ± 0.6 m, respectively.

Seasonal fluctuations in *pH* values are observed in the Ejina Delta, showing a slight increase in autumn (approximately 8.0), except for the Middle Gobi region where the trend is less pronounced. In spring, major ion concentrations generally exhibit a tendency to be lower (excluding K^+), while reaching their peak in summer (except for Ca^{2+} and HCO_3^-, which peak in autumn).

4 Discussion

4.1 Human activities amplifying interregional disparities in groundwater chemistry

In arid inland river basins, groundwater and river water are vital for sustaining desert riparian ecosystems and agricultural

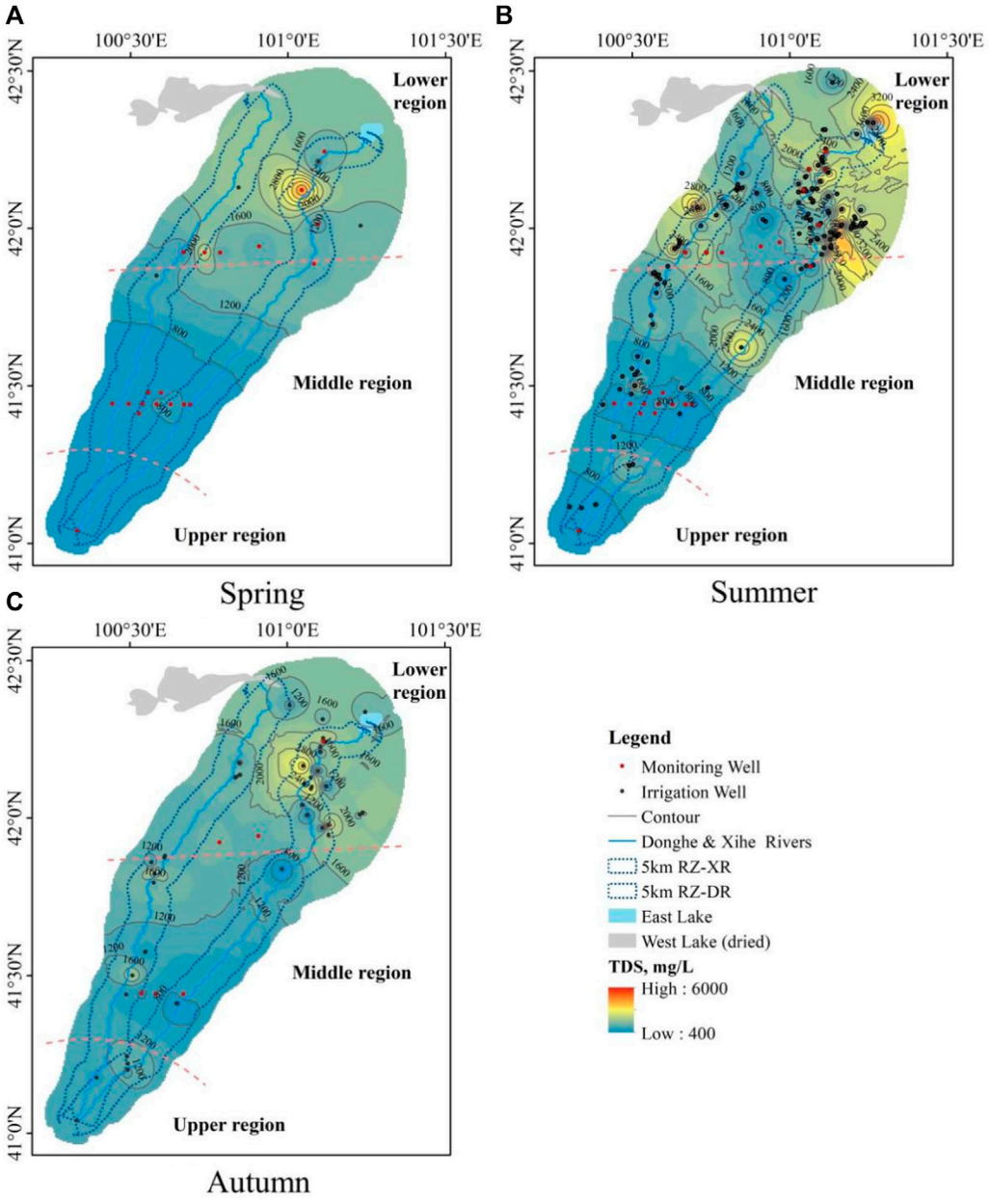

FIGURE 5
Seasonal variation of *TDS* concentration in the Ejina Delta. **(A–C)** respectively represent the variation of TDS concentration in spring, summer, and autumn.

irrigation (Huang et al., 2020; Hu Y. et al., 2021). Human activities and natural hydrological conditions are the key determinants of groundwater level and quality (Mi et al., 2016; Kou et al., 2019; Wang et al., 2019). Previous studies have indicated that *EWC* replenishes riparian shallow groundwater (Liu et al., 2022) and improves groundwater quality (Chen et al., 2005; Wang et al., 2019), while agricultural irrigation leads to groundwater depletion and water quality degradation, as well as alters the hydrogeochemical processes of groundwater (Fan et al., 2022; Yan et al., 2023). However, our results reveal significant spatial variations in the response of different zones within the Ejina Delta to these human activities.

4.1.1 Spatial variability in groundwater TDS responses to EWC

Differing from the predominantly fresh water in the Heihe River, characterized by *TDS* concentrations around 354.0 ± 157.4 mg/L (Kou et al., 2019), the Ejina Delta features elevated *TDS* concentrations in groundwater, measuring 1,527.4 ± 1,059.5 mg/L (Table 1). Consequently, a distinct spatial gradient variation in regional groundwater depth and salinity is evident (Wang W. et al., 2023), with a gradual increase from the upper region, riparian zones, and Middle Gobi towards the lower region (Supplementary Figure S4). During the period of 2001–2023, the average *TDS* concentration in the groundwater of lower region has exceeded that of the upper region, reaching up to 2.2 times higher.

Moreover, the upper region and riparian zones demonstrate as responsive areas sensitive to *EWC*, displaying distinct and regular fluctuations in groundwater salinity. As a result, the *TDS* and major ion concentrations in the upstream and Xihe zones have experienced a notable decrease from 2001 to 2023 via river influence (Supplementary Table S2). It is worth noting that, despite the fact that the annual average discharge in the Donghe River (14.2 m^3/s) can be 2.5 times that of the Xihe River (5.6 m^3/s) during 1988–2020 (Zhang J. et al., 2023), its groundwater *TDS* concentration does not exhibit a declining trend, as observed in the Xihe river. Instead, it shows a more complex pattern, indicating that, in addition to *EWC*, the groundwater chemical characteristics could be subject to additional factors, such as differences in subsurface flow pathways and geological conditions (Figures 2B, C), as elucidated by Xi et al. (2010a). The distribution and water chemistry characteristics of groundwater between these zones can also be discerned through ecosystem, which is highly sensitive to *EWC* in arid inland river basins (Huang et al., 2020; Qiu et al., 2023).

Conversely, primarily governed by groundwater evaporation and lateral recharge (Wang et al., 2014), the groundwater *TDS* concentration in the Middle Gobi has remained relatively stable, indicating a less responsive zone to *EWC*. Meanwhile, due to the concurrent influence of human activities such as irrigation in the lower region (Wang Y. et al., 2022; Wang W. et al., 2023), the direct impact of *EWC* on groundwater quality cannot be conclusively identified, the expected changes in groundwater *TDS* concentrations and its impacts on ecological system under *EWC* needs more detailed groundwater evolution model analyses.

4.1.2 Groundwater TDS responses to irrigation in lower region

From the perspective of groundwater storage (GWS), the southwestern region of the Alxa Plateau is experiencing strongly depletion due to long-term groundwater extraction, while the northwestern area (Ejina Delta) benefits from water diversion projects, groundwater depletion has been relieved (Wang et al., 2019). However, contrasting the groundwater characteristics between irrigation and non-irrigation periods reveals that agricultural water usage also exerts varying degrees of influence on groundwater in different zones of the Ejina Delta. Groundwater *TDS* is higher during irrigation periods by approximately 17% compared to non-irrigation periods in the lower region and Donghe zone, accompanied by a decrease in *WTD*. Conversely, the upstream exhibits the opposite trend, while the *TDS* difference in the Xihe and Middle Gobi areas is relatively insignificant (Supplementary Table S3).

This result confirms that long-term development of irrigation could locally contribute to a decrease in *WTD* in arid inland river basins (Ainiwaer et al., 2019; Wang W. et al., 2023), thereby facilitating salt intrusion from the vadose zone into shallow groundwater aquifers and promoting groundwater salinization (Li et al., 2016). Therefore, the groundwater *TDS* concentration is highest in the lower region across the Ejina Delta, ranging from 1,953.6 ± 1,208.5 mg/L during 2001–2023, peaking at approximately 3,000 mg/L in 2017. Simultaneously, the groundwater table in this region was the lowest (*WTD* around 4.6 ± 2.7 m), which even reached a depth of 6.3 m in 2011. As groundwater can be recharged by ephemeral runoff seepage, irrigation return flow, and subsurface lateral inflow (Wang W. et al., 2023), irrigation plays a pivotal role in the extended phreatic water recharge to groundwater (Meredith and Blais, 2019), assuming a critical function in sustaining agricultural production and fostering community stability in arid regions (Fernald et al., 2015). However, groundwater depth, salinity, and major ion concentrations could notably impact the composition and distribution of the plant community (Zeng et al., 2020). The *Populus euphratica* population exhibits a declining trend under higher salinity environments (Zhang Y. et al., 2023). Consequently, changes in groundwater *TDS* resulting from irrigation could have indirect effects on ecosystem development.

4.2 Water-rock interaction mechanisms constrain regional groundwater hydrochemical processes

The groundwater chemistry characteristics in the Ejina Delta are primarily governed by water-rock interactions and evaporation-crystallization processes, with a relatively weak seasonal variability (Figure 6). While the upper region is dominated by rock interactions (Figure 6D), other areas experience the combined influence of both processes. Notably, the lower region exhibits a stronger influence of evaporation compared to other zones (Figure 6F).

In addition, a significant shift in the dominant hydrochemical type across the Ejina Delta has been observed (Supplementary Table S2). Specifically, there is a transition from the Na-Mg-SO_4-HCO_3; Na-Mg-Ca-SO_4-HCO_3 types in the upper region to Na-Mg-SO_4-HCO_3; Na-Mg-SO_4-Cl types in the lower region. The hydrochemical composition shifted to predominantly Na-SO_4-Cl in the Middle Gobi, indicating a complex pattern of hydrochemical type transformation. Besides the pronounced influence of intense evaporation, dilution, and human activities such as agricultural drainage, the groundwater chemical characteristics are also significantly controlled by mixing and water-rock interaction (Wang W. et al., 2023). Therefore, we elucidate the hydrochemical processes underlying the observed water compositions through ionic ratio plots as indicated by Hagedorn and Whittier (2015), encompassing phenomena such as mixing, ion exchange, and chemical reactions.

The high groundwater Na/Cl ratios shown in Figure 7A serve as indicators of robust water-rock interactions (Zhu et al., 2007), with Na^+ originating not only from halite dissolution (*SI* of NaCl: −5.83 to −6.81; Supplementary Table S4 Eq. 1), but also potentially from silicate weathering and cation exchange processes (Ibe and Ebe, 2000). Among these, the Middle Gobi, Donghe and Xihe zones exhibit relatively strong water-rock interactions with Na/Cl values of 2.2, 1.9 and 2.0, respectively. In contrast, the interactions are weaker in the upper and lower regions (Na/Cl = 1.5 and 1.8, respectively). Moreover, Zhang et al. (2021) demonstrated that an excess of combined Mg^{2+} and Ca^{2+} concentrations over HCO_3^- in groundwater (Figure 7C) suggests the potential contribution of gypsum ($CaSO_4$) dissolution to the presence of Ca^{2+}. Additionally, the significant positive correlation between SO_4^{2-} and Ca^{2+} ($R^2 = 0.78$, $p < 0.01$) in Supplementary Table S5 strengthens this observation. This suggests that, along with the dissolution of carbonate minerals (calcite and dolomite), Mg^{2+} and

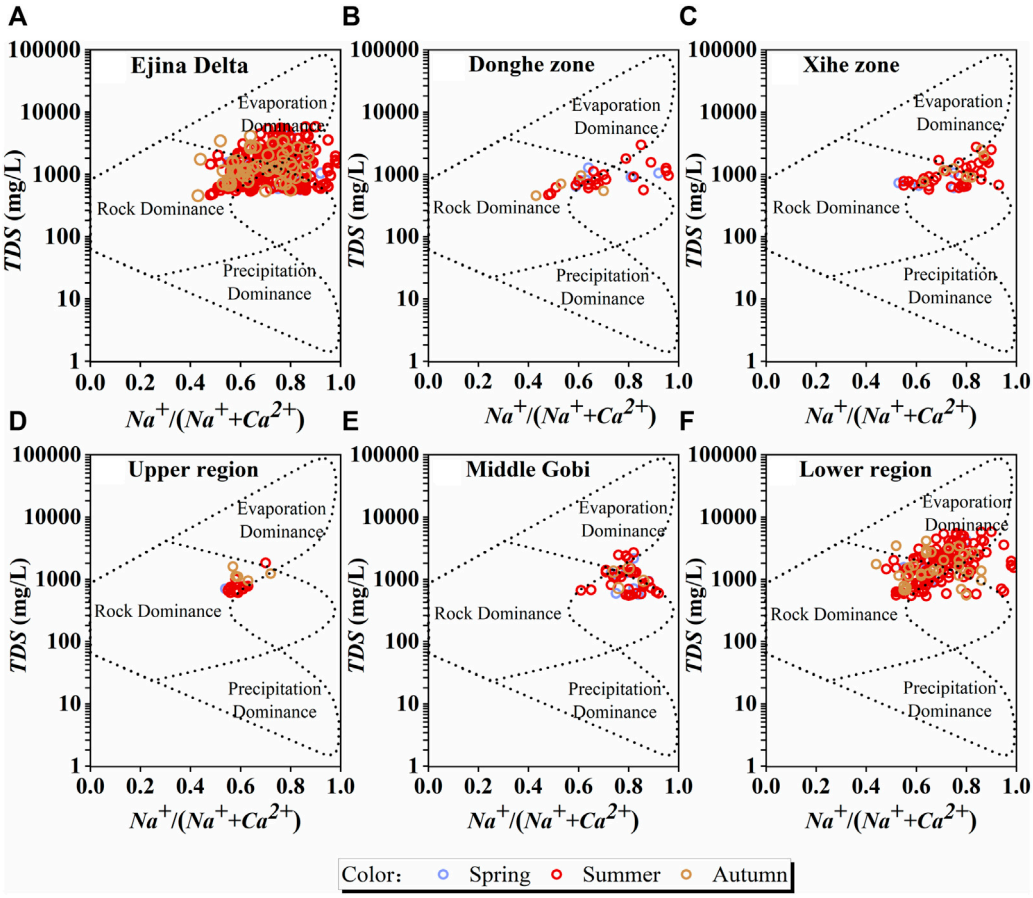

FIGURE 6
Gibbs (1970) diagrams of the processes controlling groundwater hydrochemistry. **(A–F)** respectively represent Gibbs diagrams for the Ejina Delta, Donghe zone, Xihe zone, Upper region, Middle Gobi, and Lower region.

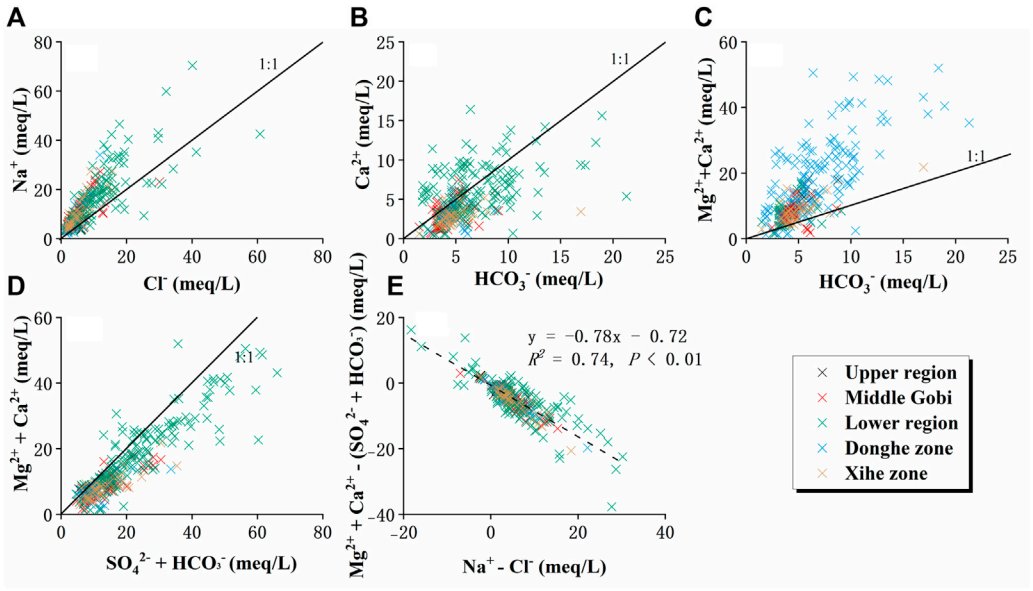

FIGURE 7
Ionic ratio plots illustrating hydrochemical processes across the Ejina Delta. (A–E) respectively represent different Ionic ratio plots.

TABLE 3 Inverse modelling of selected flow path across the Ejina Delta during the non-irrigation spring period (concentrations in mmol/L).

Path	U-X	U-M	U-D	X-L	M-LM 1	M-LM 2	D-LM	LM-L
Monitoring wells	I1 to II2	I1 to II3	I1 to II7	I2 to II1	I3 to II3	I3 to II5	I7 to II5	I5 to II2
Calcite	2.41	2.56	0.73	−2.87	−1.59	−2.84	−1.01	−1.75
CO_2(g)	−0.21	−0.67	0.16	0.36	0.63	0.06	−0.76	6.18
Dolomit	−1.23	−1.35	−0.26	1.62	0.93	1.35	0.26	2.86
Gypsum	−0.52	−0.48	−0.23	1.32	3.61	2.97	2.72	0.81
Halite	−0.08	−0.16	−0.55	0.72	3.08	2.72	3.11	−0.43
Sylvite	−0.01	0.07	−0.02	0.04	0.06	0.03	0.11	0.06
CaX_2	−1.17	−0.64	−0.13	−0.06	−1.74	−2.33	−2.85	1.30
NaX	2.33	1.28	0.25	0.12	3.48	4.66	5.70	−2.59

Note: Positive values (in black)—mineral dissolution, negative values (in red)—mineral precipitation. The T_w used in the simulation corresponds to the monthly mean values recorded by automatic monitoring wells. The selected simulation points and flow paths are depicted in Figure 2.

Ca^{2+} in groundwater also originate from the dissolution of evaporites such as gypsum ($CaSO_4$), resulting in a relatively balanced ratio of $(Mg^{2+}+Ca^{2+})/(SO_4^{2-}+HCO_3^-)$ (Figure 7D).

Furthermore, as indicated by Jankowski and Acworth (1997), the linear regression slope of $(Mg^{2+}+Ca^{2+} - (SO_4^{2-}+HCO_3^-))/(Na^+-Cl^-)$ ratio of −0.78 in the Ejina Delta implies the involvement of cation exchange reactions in groundwater hydrogeochemical processes (Figure 7E). Therefore, a more comprehensive understanding of the groundwater hydrochemical evolution requires a quantitative analysis of the spatial variations in water-rock interaction processes across the Ejina Delta.

4.3 Hydrogeochemical process revealed by inverse geochemical modelling

Through inverse modelling using PHREEQC based on data from 13 monitoring wells, which is characterized by groundwater chemistry that is consistent with the overall Ejina Delta chemistry (Supplementary Figures S5, S6). We found that the groundwater across the study area exhibits quasi-equilibrium conditions for calcite (*SI*: −0.28 ~ 0.27) and dolomite (*SI*: −0.31 ~ 0.77), with an observed transition between oversaturation and undersaturation (Supplementary Table S4). Furthermore, Gypsum (*SI*: −1.68 ~ −0.85), rock salt (*SI*: −6.81 ~ −5.83), and potash salt (*SI*: −7.42 ~ −6.74) exhibit undersaturation conditions, with a decreasing trend in *SI* towards the lower region, implying strong evaporation-crystallization processes under the arid environment (Shen et al., 2021), or a potential dissolution trend for these minerals along the groundwater pathway.

Based on the results of inverse modeling along the selected flow path across the Ejina Delta, the calcite dissolution and precipitation of dolomite, gypsum, halite, and sylvite salts, as well as cation exchange reactions ($2NaX+Ca^{2+}\rightarrow CaX_2+2Na^+$) were observe from the upper region to the Middle Gobi and riparian zones (U-X, U-M, U-D in Table 3). This trend led to an increase in concentrations of HCO_3^- and Na^+ in groundwater, while other major ion concentrations decreased along the flow path (Supplementary Table S6). In contrast, water-rock interactions exhibited an opposite pattern from the middle to the lower region (Table 3), involving calcite precipitation and dissolution of dolomite, gypsum, halite, and sylvite salts. This trend resulted in a significant increase in major ions and *TDS* concentrations in the lower region (Supplementary Table S6), accompanied by the intensification of evaporation processes (Figure 6F).

It is noteworthy that along the LM-L flow path, Point VIII2—located near the farmland in the downstream area (Figure 1)—is characterized by unique water-rock interaction phenomena, influenced by anthropogenic activities such as surface water flood irrigation. These phenomena include distinctive cation exchange reactions (with changes in NaX and CaX_2 concentrations of −2.59 mmol/L and 1.30 mmol/L, respectively), halite precipitation (a reduction in halite by 0.43 mmol/L), carbon dioxide absorption (an increase in CO_2 by 6.18 mmol/L), and elevated concentrations of major ions and *TDS* in the groundwater.

In summary, the intrinsic mechanisms of complex groundwater variations, including *WTD*, *TDS* concentration and hydrochemical types across the entire Ejina Delta, are significant intricate (Figure 8). The *EWC* process plays a crucial role in temporally replenishing and diluting groundwater in the upper region and riparian zones, influencing interactions between groundwater and surface-water (Mi et al., 2016; Yuan et al., 2020). This dynamic, combined with the slow movement of groundwater in the upper-middle region of the Ejina Delta, facilitates the effective dissolution of calcite during vertical recharge and transport (Liu Y. et al., 2018). Simultaneously, in the middle-lower region under the impact of evapotranspiration (*ET*) (Li et al., 2012) and relatively weaker impact of *EWC*, leads to a notable decrease in the proportion of Ca^{2+} and an increase in Cl^- among all ions. This is probably attributed to water-rock interactions, involving the precipitation of calcite and CaX_2, and the dissolution of halite in the middle-lower region. In the lower region, escalating human activities are progressively increasing groundwater salinity, influenced by a composite interplay of natural processes (e.g., evaporation) and human activities (e.g., *EWC* and irrigation as indicated by Yang et al. (2018)). It is noteworthy that agricultural irrigation, by reducing the *WTD*, can also promote evaporation-crystallization processes (Wang et al., 2020). However, due to the heterogeneity of subsurface geological conditions, variations in water-rock interactions and

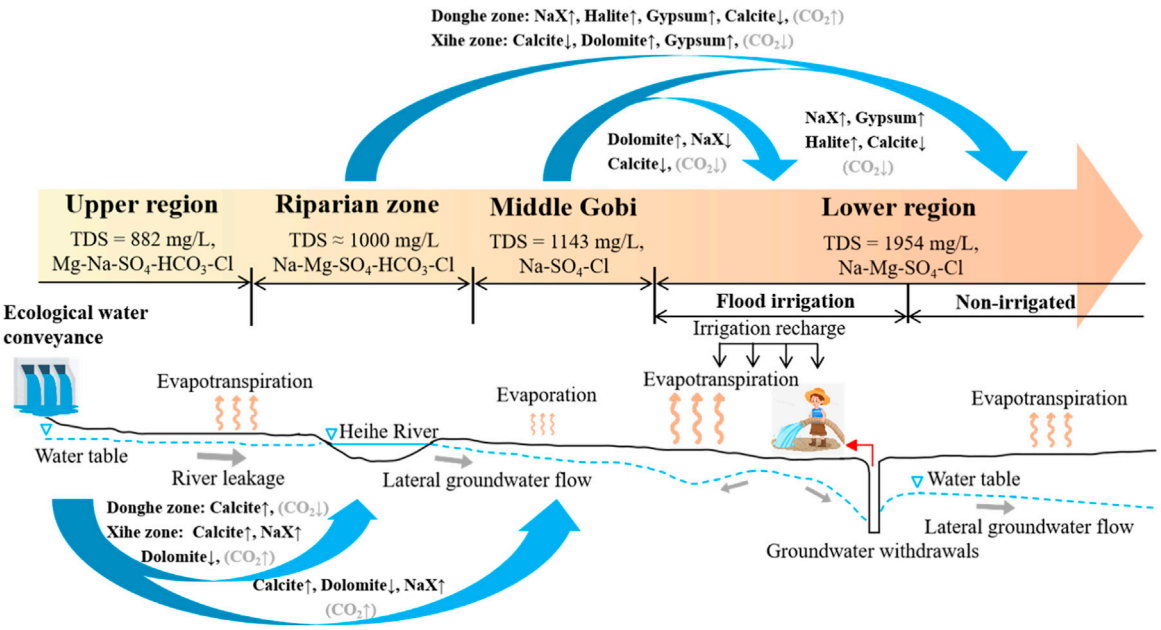

FIGURE 8
Hydrogeochemical evolution scheme of groundwater in the Ejina Delta.

groundwater characteristics differ along various zones. This necessitates a more systematic approach to sampling and modelling.

5 Conclusion

In this study, we sought to identify the spatiotemporal variation of groundwater hydrogeochemistry across the Ejina Delta and reveal the potential mechanism on the variations in the salinity and water types of different zones. We found that the groundwater salinity increases from upper to lower region under the impact of both natural processes and human activities. The former primarily influences water levels and quality by enhancing the interaction between surface water and groundwater, resulting in a decreasing trend in groundwater *TDS* concentrations in the upper region and Xihe zone during 2001–2023. While, human activities such as *EWC* and agricultural irrigation alter the hydrogeochemical processes of the groundwater in arid inland river basins, and are more pronounced in downstream areas, which reduces the *WTD* and affects evaporation-crystallization processes, thus intensifying salinization in the groundwater of the lower region.

We further identified the influence of water-rock interactions on groundwater hydrochemical characteristic and concluded that shifts in groundwater types are likely attribute to mineral dissolution and precipitation. Despite the inherent complexity of the process driving groundwater hydrochemistry, our efforts were directed towards revealing the impact of both rock and evaporation dominant processes on the groundwater composition across the Ejina Delta. Human activities could alter groundwater chemical processes by influencing the conditions of water-rock interactions, including geological conditions, lithological composition, groundwater connectivity, etc. *EWC*, to some extent, facilitated water-rock interactions via the lateral flow of groundwater, whereas irrigation has disrupted the natural hydrogeochemical equilibrium. In arid regions, it is essential to consider the impact of irrigation on groundwater chemistry, as well as the differences in geological conditions and their influence on groundwater chemistry through water-rock interactions.

Notably, our analysis did not consider the impact of solutes stored in the vadose zone (Min et al., 2018), ecosystem changes under *EWC* (Hu S. et al., 2021; Li et al., 2022), local mining industry, upstream water resources management (Xi et al., 2010b) on groundwater hydrogeochemistry. Nevertheless, our study on inverse modelling of groundwater hydrogeochemical evolution process provides a current overview of the water-rock interaction within the Ejina Delta and reveals its heterogeneity. More detailed data on groundwater chemistry, coupled with the application of machine learning models (Haggerty et al., 2023), as well as establishing a network for long-term, continuous monitoring of groundwater variations, are critically important. The findings of this study offer a theoretical foundation for elucidating the anthropogenic and natural processes that govern changes in groundwater quality, thereby facilitating the optimization of water resource allocation and the management of groundwater quality in arid regions.

Data availability statement

The raw data supporting the conclusion of this article will be made available by the authors, without undue reservation.

Author contributions

JZ: Data curation, Formal Analysis, Investigation, Writing–original draft. PW: Conceptualization, Funding acquisition, Methodology, Supervision, Writing–original draft. SL: Methodology, Writing–original draft. JY: Writing–review and editing.

Funding

The author(s) declare that financial support was received for the research, authorship, and/or publication of this article. This research was funded by the National Natural Science Foundation of China (Nos. 42071042, 42061134017) and the National Key Research and Development Program of China (Nos. 2023YFC3206803, 2023YFC3206801).

Conflict of interest

The authors declare that the research was conducted in the absence of any commercial or financial relationships that could be construed as a potential conflict of interest.

Publisher's note

All claims expressed in this article are solely those of the authors and do not necessarily represent those of their affiliated organizations, or those of the publisher, the editors and the reviewers. Any product that may be evaluated in this article, or claim that may be made by its manufacturer, is not guaranteed or endorsed by the publisher.

Supplementary material

The Supplementary Material for this article can be found online at: https://www.frontiersin.org/articles/10.3389/fenvs.2024.1376443/full#supplementary-material

References

Ainiwaer, M., Ding, J., Wang, J., and Nasierding, N. (2019). Spatiotemporal dynamics of water table depth associated with changing agricultural land use in an arid zone oasis. *Water* 11 (4), 673. doi:10.3390/w11040673

Akiyama, T., Sakai, A., Yamazaki, Y., Wang, G., Fujita, K., Nakawo, M., et al. (2007). Surface water-groundwater interaction in the Heihe River basin, northwestern China. *Bull. Glaciol. Res.* 24, 87–94.

Asubiojo, O. I., Nkono, N. A., Ogunsua, A. O., Oluwole, A. F., Ward, N. I., Akanle, O. A., et al. (1997). Trace elements in drinking and groundwater samples in Southern Nigeria. *Sci. Total Environ.* 208 (1-2), 1–8. doi:10.1016/s0048-9697(97)00178-2

Chen, W., Wang, J., Ding, J., Ge, X., Han, L., and Qin, S. (2023). Detecting long-term series eco-environmental quality changes and driving factors using the remote sensing ecological index with salinity adaptability (rseisi): a case study in the Tarim River basin, China. *Land* 12, 1309. doi:10.3390/land12071309

Chen, Y., Chen, Y., Liu, J., Li, W., Li, J., and Xu, C. (2005). Dynamical variations in groundwater chemistry influenced by intermittent water delivery at the lower reaches of the Tarim River. *J. Geogr. Sci.* 15 (1), 13–19. doi:10.1360/gs050102

Chen, Y., Chen, Y., Zhu, C., Wang, Y., and Hao, X. (2022). Ecohydrological effects of water conveyance in a disconnected river in an arid inland river basin. *Sci. Rep.* 12 (1), 9982. doi:10.1038/s41598-022-14524-z

Cheng, G., Li, X., Zhao, W., Xu, Z., Feng, Q., Xiao, S., et al. (2014). Integrated study of the water–ecosystem–economy in the Heihe River Basin. *Natl. Sci. Rev.* 1, 413–428. doi:10.1093/nsr/nwu017

Döll, P., Hoffmann-Dobrev, H., Portmann, F. T., Siebert, S., Eicker, A., Rodell, M., et al. (2012). Impact of water withdrawals from groundwater and surface water on continental water storage variations. *J. Geodyn.* 59–60 (0), 143–156. doi:10.1016/j.jog.2011.05.001

Du, C., Yu, J., Wang, P., and Zhang, Y. (2016). Reference evapotranspiration changes: sensitivities to and contributions of meteorological factors in the Heihe River basin of northwestern China (1961-2014). *Adv. Meteorology* 2016, 1–17. doi:10.1155/2016/4143580

Famiglietti, J. S. (2014). The global groundwater crisis. *Nat. Clim. Change* 4 (11), 945–948. doi:10.1038/nclimate2425

Fan, G., Zhang, D., Zhang, J., Li, Z., Sang, W., Zhao, L., et al. (2022). Ecological environmental effects of Yellow River irrigation revealed by isotope and ion hydrochemistry in the Yinchuan Plain, Northwest China. *Ecol. Indic.* 135, 108574. doi:10.1016/j.ecolind.2022.108574

Fang, Y., Wang, X., Cheng, Y., and Wang, Z. (2022). Oasis change characteristics and influencing factors in the Shiyang River basin, China. *Sustainability* 14 (21), 14354. doi:10.3390/su142114354

Fernald, A., Guldan, S., Boykin, K., Cibils, A., Gonzales, M., Hurd, B., et al. (2015). Linked hydrologic and social systems that support resilience of traditional irrigation communities. *Hydrol. Earth Syst. Sci.* 19 (1), 293–307. doi:10.5194/hess-19-293-2015

Gibbs, R. J. (1970). Mechanisms controlling world water chemistry. *Science* 170 (3962), 1088–1090. doi:10.1126/science.170.3962.1088

Guo, X., Feng, Q., Si, J., Xi, H., Zhao, Y., and Deo, R. C. (2019). Partitioning groundwater recharge sources in multiple aquifers system within a desert oasis environment: implications for water resources management in endorheic basins. *J. Hydrology* 579, 124212. doi:10.1016/j.jhydrol.2019.124212

Hagedorn, B., and Whittier, R. B. (2015). Solute sources and water mixing in a flashy mountainous stream (Pahsimeroi River, US Rocky Mountains): implications on chemical weathering rate and groundwater-surface water interaction. *Chem. Geol.* 391, 123–137. doi:10.1016/j.chemgeo.2014.10.031

Haggerty, R., Sun, J., Yu, H., and Li, Y. (2023). Application of machine learning in groundwater quality modeling-A comprehensive review. *Water Res.* 233, 119745. doi:10.1016/j.watres.2023.119745

Helena, B., Pardo, R., Vega, M., Barrado, E., Fernandez, J. M., and Fernandez, L. (2000). Temporal evolution of groundwater composition in an alluvial aquifer (Pisuerga River, Spain) by principal component analysis. *Water Res.* 34 (3), 807–816. doi:10.1016/s0043-1354(99)00225-0

Hu, K. X., Awange, J. L., Kuhn, M., and Saleem, A. (2019). Spatio-temporal groundwater variations associated with climatic and anthropogenic impacts in South-West Western Australia. *Sci. Total Environ.* 696, 133599. doi:10.1016/j.scitotenv.2019.133599

Hu, S., Ma, R., Sun, Z., Ge, M., Zeng, L., Huang, F., et al. (2021a). Determination of the optimal ecological water conveyance volume for vegetation restoration in an arid inland river basin, northwestern China. *Sci. Total Environ.* 788, 147775. doi:10.1016/j.scitotenv.2021.147775

Hu, Y., Lu, Y., Edmonds, J., Liu, C., Zhang, Q., and Zheng, C. (2021b). Irrigation alters source-composition characteristics of groundwater dissolved organic matter in a large arid river basin, Northwestern China. *Sci. Total Environ.* 767, 144372. doi:10.1016/j.scitotenv.2020.144372

Huang, F., Chunyu, X., Zhang, D., Chen, X., and Ochoa, C. G. (2020). A framework to assess the impact of ecological water conveyance on groundwater-dependent terrestrial ecosystems in arid inland river basins. *Sci. Total Environ.* 709, 136155. doi:10.1016/j.scitotenv.2019.136155

Huang, M.-T., and Zhai, P.-M. (2023). Desertification dynamics in China's drylands under climate change. *Adv. Clim. Change Res.* 14 (3), 429–436. doi:10.1016/j.accre.2023.05.001

Huo, Z., Feng, S., Kang, S., Li, W., and Chen, S. (2008). Effect of climate changes and water-related human activities on annual stream flows of the Shiyang river basin in arid north-west China. *Hydrol. Process.* 22 (16), 3155–3167. doi:10.1002/hyp.6900

Ibe, K. M., and Ebe, A. M. (2000). Impacts of debris-flow deposits on hydrogeochemical processes and the development of dryland salinity in the Cross-River catchment, SE, Nigeria. *Environ. Monit. Assess.* 64 (2), 449–456. doi:10.1023/a:1006352922219

Jankowski, J., and Acworth, R. I. (1997). Impact of debris-flow deposits on hydrogeochemical processes and the developement of dryland salinity in the yass river catchment, new south wales, Australia. *Hydrogeology J.* 5 (4), 71–88. doi:10.1007/s100400050119

Jiang, C., Cheng, L., Li, C., and Zheng, L. (2022). A hydrochemical and multi-isotopic study of groundwater sulfate origin and contribution in the coal mining area. *Ecotoxicol. Environ. Saf.* 248, 114286. doi:10.1016/j.ecoenv.2022.114286

Jiang, X., Xia, J., Huang, Q., Long, A., Dong, G., and Song, J. (2019). Adaptability analysis of the Heihe River "97" water diversion scheme. *Acta Geogr. Sin.* 74 (01), 103–116. doi:10.11821/dlxb201901008

Jiang, X. H., and Liu, C. M. (2010). The influence of water regulation on vegetation in the lower Heihe River. *J. Geogr. Sci.* 20 (5), 701–711. doi:10.1007/s11442-010-0805-6

Karunanidhi, D., Aravinthasamy, P., Deepali, M., Subramani, T., and Roy, P. D. (2020). The effects of geochemical processes on groundwater chemistry and the health risks associated with fluoride intake in a semi-arid region of South India. *Rsc Adv.* 10 (8), 4840–4859. doi:10.1039/c9ra10332e

Kou, Y., Li, Z., Hua, K., and Li, Z. (2019). Hydrochemical characteristics, controlling factors, and solute sources of streamflow and groundwater in the Hei River catchment, China. *China. Water* 11 (11), 2293. doi:10.3390/w11112293

Labarca, F., and Borquez, R. (2020). Comparative study of nanofiltration and ion exchange for nitrate reduction in the presence of chloride and iron in groundwater. *Sci. Total Environ.* 723, 137809. doi:10.1016/j.scitotenv.2020.137809

Li, L., Jiang, E., Yin, H., Wu, K., and Dong, G. (2022). Ultrashort-term responses of riparian vegetation restoration to adjacent cycles of ecological water conveyance scheduling in a hyperarid endorheic river basin. *J. Environ. Manag.* 320, 115803. doi:10.1016/j.jenvman.2022.115803

Li, X., Cheng, G., Ge, Y., Li, H., Han, F., Hu, X., et al. (2018). Hydrological cycle in the Heihe River basin and its implication for water resource management in endorheic basins. *J. Geophys. Res. Atmos.* 123 (2), 890–914. doi:10.1002/2017jd027889

Li, X., Jin, M., Zhou, N., Huang, J., Jiang, S., and Telesphore, H. (2016). Evaluation of evapotranspiration and deep percolation under mulched drip irrigation in an oasis of Tarim basin, China. *J. Hydrology* 538, 677–688. doi:10.1016/j.jhydrol.2016.04.045

Li, X., Lu, L., Yang, W., and Cheng, G. (2012). Estimation of evapotranspiration in an arid region by remote sensing-A case study in the middle reaches of the Heihe River Basin. *Int. J. Appl. Earth Observation Geoinformation* 17, 85–93. doi:10.1016/j.jag.2011.09.008

Liu, M., Jiang, Y., Xu, X., Huang, Q., Huo, Z., and Huang, G. (2018a). Long-term groundwater dynamics affected by intense agricultural activities in oasis areas of arid inland river basins, Northwest China. *Agric. Water Manag.* 203, 37–52. doi:10.1016/j.agwat.2018.02.028

Liu, Q., Gui, D., Zhang, L., Niu, J., Dai, H., Wei, G., et al. (2022). Simulation of regional groundwater levels in arid regions using interpretable machine learning models. *Sci. Total Environ.* 831, 154902. doi:10.1016/j.scitotenv.2022.154902

Liu, X., Yu, J., Wang, P., Zhang, Y., and Du, C. (2016). Lake evaporation in a hyper-arid environment, northwest of China-measurement and estimation. *Water* 8 (11), 527. doi:10.3390/w8110527

Liu, Y., Jin, M., and Wang, J. (2018b). Insights into groundwater salinization from hydrogeochemical and isotopic evidence in an arid inland basin. *Hydrol. Process.* 32 (20), 3108–3127. doi:10.1002/hyp.13243

Liu, Y., Wang, P., Gojenko, B., Yu, J., Wei, L., Luo, D., et al. (2021). A review of water pollution arising from agriculture and mining activities in Central Asia: facts, causes and effects. *Environ. Pollut.* 291, 118209. doi:10.1016/j.envpol.2021.118209

Liu, Y., Wei, L., Deng, H., Hu, S., Xie, X., Luo, D., et al. (2023). Hydrogeochemistry of groundwater surrounding a pyrite mine in southern China: assessment of the diffusive gradients in thin films technique for *in situ* monitoring. *J. Hydrology* 622, 129685. doi:10.1016/j.jhydrol.2023.129685

Ma, J. Z., Wang, X. S., and Edmunds, W. M. (2005). The characteristics of groundwater resources and their changes under the impacts of human activity in the arid Northwest China - a case study of the Shiyang River Basin. *J. Arid Environ.* 61 (2), 277–295. doi:10.1016/j.jaridenv.2004.07.014

Marandi, A., and Shand, P. (2018). Groundwater chemistry and the gibbs diagram. *Appl. Geochem.* 97, 209–212. doi:10.1016/j.apgeochem.2018.07.009

Mensah, J. K., Ofosu, E. A., Yidana, S. M., Akpoti, K., and Kabo-bah, A. T. (2022). Integrated modeling of hydrological processes and groundwater recharge based on land use land cover, and climate changes: a systematic review. *Environ. Adv.* 8, 100224. doi:10.1016/j.envadv.2022.100224

Meredith, E., and Blais, N. (2019). Quantifying irrigation recharge sources using groundwater modeling. *Agric. Water Manag.* 214, 9–16. doi:10.1016/j.agwat.2018.12.032

Meredith, K. T., Hollins, S. E., Hughes, C. E., Cendón, D. I., Hankin, S., and Stone, D. J. M. (2009). Temporal variation in stable isotopes (18O and 2H) and major ion concentrations within the Darling River between Bourke and Wilcannia due to variable flows, saline groundwater influx and evaporation. *J. Hydrology* 378 (3), 313–324. doi:10.1016/j.jhydrol.2009.09.036

Mi, L., Xiao, H., Zhang, J., Yin, Z., and Shen, Y. (2016). Evolution of the groundwater system under the impacts of human activities in middle reaches of Heihe River Basin (Northwest China) from 1985 to 2013. *Hydrogeology J.* 24 (4), 971–986. doi:10.1007/s10040-015-1346-y

Min, L., Shen, Y., Pei, H., and Wang, P. (2018). Water movement and solute transport in deep vadose zone under four irrigated agricultural land-use types in the North China Plain. *J. Hydrology* 559, 510–522. doi:10.1016/j.jhydrol.2018.02.037

Parkhurst, D. L., and Appelo, C. A. J. (1999). User's guide to PHREEQC-A computer program for speciation, reaction-path, 1D-transport, and inverse geochemical calculations. *U. S. Geol. Surv. Water-Resources Investig. Rep.* 99, 4259. doi:10.3133/wri994259

Parkhurst, D. L., and Appelo, C. A. J. (2013) *Description of input and examples for PHREEQC Version 3: a computer program for speciation, batch-reaction, one-dimensional transport, and inverse geochemical calculations*. Reston, VA: US Geological Survey Techniques and Methods.

Peng, X., Xiao, S., Yang, B., and Yu, T. (2022). Water allocation and climate-impacted riparian forest dynamics in the Ejina Oasis, Northwest China. *Dendrochronologia* 76, 126001. doi:10.1016/j.dendro.2022.126001

Petch, S., Dong, B., Quaife, T., King, R. P., and Haines, K. (2023). Precipitation explains GRACE water storage variability over large endorheic basins in the 21st century. *Front. Environ. Sci.* 11. doi:10.3389/fenvs.2023.1228998

Piper, A. M. (1944). A graphic procedure in the geochemical interpretation of water-analyses. *Transactions-American Geophys. Union* 25, 914–923. doi:10.1029/TR025i006p00914

Qian, K., Ma, X., Yan, W., Li, J., Xu, S., Liu, Y., et al. (2024). Trade-offs and synergies among ecosystem services in Inland River Basins under the influence of ecological water transfer project: a case study on the Tarim River basin. *Sci. Total Environ.* 908, 168248. doi:10.1016/j.scitotenv.2023.168248

Qin, D., Zhao, Z., Han, L., Qian, Y., Ou, L., Wu, Z., et al. (2012). Determination of groundwater recharge regime and flowpath in the Lower Heihe River basin in an arid area of Northwest China by using environmental tracers: implications for vegetation degradation in the Ejina Oasis. *Appl. Geochem.* 27 (6), 1133–1145. doi:10.1016/j.apgeochem.2012.02.031

Qin, K., Zhao, Q., Yu, H., Li, J., Jiang, J., Wang, K., et al. (2021). Removal trend of amoxicillin and tetracycline during groundwater recharging reusing: redox sensitivity and microbial community response. *Chemosphere* 282, 131011. doi:10.1016/j.chemosphere.2021.131011

Qiu, D., Zhu, G., Bhat, M. A., Wang, L., Liu, Y., Sang, L., et al. (2023). Water use strategy of nitraria tangutorum shrubs in ecological water delivery area of the lower inland river: based on stable isotope data. *J. Hydrology* 624, 129918. doi:10.1016/j.jhydrol.2023.129918

Rajmohan, N., Masoud, M. H. Z., and Niyazi, B. A. M. (2021). Impact of evaporation on groundwater salinity in the arid coastal aquifer, Western Saudi Arabia. *Catena* 196, 104864. doi:10.1016/j.catena.2020.104864

Sami, K. (1992). Recharge mechanisms and geochemical processes in a semi-arid sedimentary basin, Eastern Cape, South Africa. *J. Hydrology* 139 (1), 27–48. doi:10.1016/0022-1694(92)90193-y

Scanlon, B. R., Keese, K. E., Flint, A. L., Flint, L. E., Gaye, C. B., Edmunds, W. M., et al. (2006). Global synthesis of groundwater recharge in semiarid and arid regions. *Hydrol. Process.* 20 (15), 3335–3370. doi:10.1002/hyp.6335

Shen, B. B., Wu, J. L., Zhan, S., Jin, M., Saparov, A. S., and Abuduwaili, J. (2021). Spatial variations and controls on the hydrochemistry of surface waters across the Ili-Balkhash Basin, arid Central Asia. *J. Hydrology* 600, 126565. doi:10.1016/j.jhydrol.2021.126565

Tao, H., Gemmer, M., Bai, Y., Su, B., and Mao, W. (2011). Trends of streamflow in the Tarim River Basin during the past 50years: human impact or climate change? *J. Hydrology* 400 (1), 1–9. doi:10.1016/j.jhydrol.2011.01.016

Tao, H., Gemmer, M., Song, Y., and Jiang, T. (2008). Ecohydrological responses on water diversion in the lower reaches of the Tarim River, China. *Water Resour. Res.* 44 (8). doi:10.1029/2007wr006186

Vasilevskiy, P., Wang, P., Pozdniakov, S., Wang, T., Zhang, Y., Zhang, X., et al. (2022). Simulating River/Lake–Groundwater exchanges in arid river basins: an improvement constrained by lake surface area dynamics and evapotranspiration. *Remote Sens.* 14 (7), 1657. doi:10.3390/rs14071657

Wan, L., Bento, V. A., Qu, Y., Qiu, J., Song, H., Zhang, R., et al. (2023). Drought characteristics and dominant factors across China: insights from high-resolution daily SPEI dataset between 1979 and 2018. *Sci. Total Environ.* 901, 166362. doi:10.1016/j.scitotenv.2023.166362

Wang, G., and Cheng, G. (1999). Water resource development and its influence on the environment in arid areas of China—the case of the Hei River basin. *J. Arid Environ.* 43 (2), 121–131. doi:10.1006/jare.1999.0563

Wang, J., Ma, Z., Wang, Z., Huang, X., Hou, Q., Cao, Y., et al. (2023a). Evolution of the landscape ecological pattern in arid riparian zones based on the perspective of watershed river-groundwater transformation. *J. Hydrology* 625, 130119. doi:10.1016/j.jhydrol.2023.130119

Wang, J., Song, C., Reager, J. T., Yao, F., Famiglietti, J. S., Sheng, Y., et al. (2018). Recent global decline in endorheic basin water storages. *Nat. Geosci.* 11 (12), 926–932. doi:10.1038/s41561-018-0265-7

Wang, P., Huang, Q., Liu, S., Liu, Y., Li, Z., Pozdniakov, S. P., et al. (2024). Climate warming enhances chemical weathering in permafrost-dominated eastern Siberia. *Sci. Total Environ.* 906, 167367. doi:10.1016/j.scitotenv.2023.167367

Wang, P., Pozdniakov, S. P., and Vasilevskiy, P. Y. (2017). Estimating groundwater-ephemeral stream exchange in hyper-arid environments: field experiments and numerical simulations. *J. Hydrology* 555, 68–79. doi:10.1016/j.jhydrol.2017.10.004

Wang, P., Yu, J., Pozdniakov, S. P., Grinevsky, S. O., and Liu, C. (2014). Shallow groundwater dynamics and its driving forces in extremely arid areas: a case study of the lower Heihe River in northwestern China. *Hydrol. Process.* 28 (3), 1539–1553. doi:10.1002/hyp.9682

Wang, P., Yu, J., Zhang, Y., Fu, G., Min, L., and Ao, F. (2011a). Impacts of environmental flow controls on the water table and groundwater chemistry in the Ejina Delta, northwestern China. *Environ. Earth Sci.* 64 (1), 15–24. doi:10.1007/s12665-010-0811-0

Wang, P., Yu, J., Zhang, Y., and Liu, C. (2013). Groundwater recharge and hydrogeochemical evolution in the Ejina Basin, northwest China. *J. Hydrology* 476, 72–86. doi:10.1016/j.jhydrol.2012.10.049

Wang, P., Zhang, Y., Yu, J., Fu, G., and Ao, F. (2011b). Vegetation dynamics induced by groundwater fluctuations in the lower Heihe River Basin, northwestern China. *J. Plant Ecol.* 4 (1-2), 77–90. doi:10.1093/jpe/rtr002

Wang, T., Wang, P., Zhang, Y., Yu, J., Du, C., and Fang, Y. (2019). Contrasting groundwater depletion patterns induced by anthropogenic and climate-driven factors on Alxa Plateau, northwestern China. *J. Hydrology* 576, 262–272. doi:10.1016/j.jhydrol.2019.06.057

Wang, T., Wu, Z., Wang, P., Wu, T., Zhang, Y., Yin, J., et al. (2023b). Plant-groundwater interactions in drylands: a review of current research and future perspectives. *Agric. For. Meteorology* 341, 109636. doi:10.1016/j.agrformet.2023.109636

Wang, W., Chen, Y., Wang, W., Zhu, C., Chen, Y., Liu, X., et al. (2023c). Water quality and interaction between groundwater and surface water impacted by agricultural activities in an oasis-desert region. *J. Hydrology* 617, 128937. doi:10.1016/j.jhydrol.2022.128937

Wang, X., Ge, Q., Geng, X., Wang, Z., Gao, L., Bryan, B. A., et al. (2023d). Unintended consequences of combating desertification in China. *Nat. Commun.* 14 (1), 1139. doi:10.1038/s41467-023-36835-z

Wang, X., Song, J., Xiao, Z., Wang, J., and Hu, F. (2022a). Desertification in the mu us sandy land in China: response to climate change and human activity from 2000 to 2020. *Geogr. Sustain.* 3 (2), 177–189. doi:10.1016/j.geosus.2022.06.001

Wang, Y., Li, S., Qin, S., Guo, H., Yang, D., and Lam, H.-M. (2020). How can drip irrigation save water and reduce evapotranspiration compared to border irrigation in arid regions in northwest China. *Agric. Water Manag.* 239, 106256. doi:10.1016/j.agwat.2020.106256

Wang, Y., Yuan, S., Shi, J., Ma, T., Xie, X., Deng, Y., et al. (2023e). Groundwater quality and health: making the invisible visible. *Environ. Sci. Technol.* 57 (13), 5125–5136. doi:10.1021/acs.est.2c08061

Wang, Y., Zhao, Y., Yan, L., Deng, W., Zhai, J., Chen, M., et al. (2022b). Groundwater regulation for coordinated mitigation of salinization and desertification in arid areas. *Agric. Water Manag.* 271, 107758. doi:10.1016/j.agwat.2022.107758

Wei, S., Wang, Z., Li, F., Wu, X., and Xu, R. (2023). Characteristics of hydrogen and oxygen stable isotopes and hydrochemistryin the groundwater of Ejina plain, Inner Mongolia and its hydrochemical evolution. *Geol. China* 50 (01), 159–169. doi:10.12029/gc20230112

Wen, X., Wu, Y., Su, J., Zhang, Y., and Liu, F. (2005). Hydrochemical characteristics and salinity of groundwater in the Ejina basin, northwestern China. *Environ. Geol.* 48 (6), 665–675. doi:10.1007/s00254-005-0001-7

Wu, X., Shi, S., Li, Z., Hao, A., Qiao, W., Yu, Z., et al. (2002). The study on the groundwater flow system of Ejina basin in lower reaches of the Heihe River in Northwest China (Part 1) (in Chinese with English abstract). *Hydrogeology Eng. Geol.* 1, 16–20. doi:10.3969/j.issn.1000-3665.2002.01.005

Xi, H., Feng, Q., Liu, W., Si, J., Chang, Z., and Su, Y. (2010a). The research of groundwater flow model in Ejina Basin, Northwestern China. *Environ. Earth Sci.* 60 (5), 953–963. doi:10.1007/s12665-009-0231-1

Xi, H., Feng, Q., Si, J., Chang, Z., and Cao, S. (2010b). Impacts of river recharge on groundwater level and hydrochemistry in the lower reaches of Heihe River Watershed, northwestern China. *Hydrogeology J.* 18 (3), 791–801. doi:10.1007/s10040-009-0562-8

Yan, Y., Guan, Q., Shao, W., Wang, Q., Yang, X., and Luo, H. (2023). Spatiotemporal dynamics and driving mechanism of arable ecosystem stability in arid and semi-arid areas based on Pressure-Buffer-Response process. *J. Clean. Prod.* 421, 138553. doi:10.1016/j.jclepro.2023.138553

Yang, J., Yang, K., and Wang, C. (2023). How desertification in northern China will change under a rapidly warming climate in the near future (2021–2050). *Theor. Appl. Climatol.* 151 (1), 935–948. doi:10.1007/s00704-022-04315-x

Yang, L., Zhu, G., Shi, P., Li, J., Liu, Y., Tong, H., et al. (2018). Spatiotemporal characteristics of hydrochemistry in Asian arid inland basin-a case study of Shiyang River Basin. *Environ. Sci. Pollut. Res.* 25 (3), 2293–2302. doi:10.1007/s11356-017-0504-2

Yang, Q., Xiao, H., Zhao, L., Yang, Y., Li, C., Zhao, L., et al. (2011). Hydrological and isotopic characterization of river water, groundwater, and groundwater recharge in the Heihe River basin, northwestern China. *Hydrol. Process.* 25 (8), 1271–1283. doi:10.1002/hyp.7896

Yao, Y., Zheng, C., Tian, Y., Liu, J., and Zheng, Y. (2015). Numerical modeling of regional groundwater flow in the Heihe River Basin, China: advances and new insights. *Sci. China Earth Sci.* 58 (1), 3–15. doi:10.1007/s11430-014-5033-y

Yu, H., Chen, Y., Zhou, G., and Xu, Z. (2022). Coordination of leaf functional traits under climatic warming in an arid ecosystem. *BMC Plant Biol.* 22 (1), 439. doi:10.1186/s12870-022-03818-z

Yu, J., Zhou, J., Zhao, J., Chen, R., Yao, X., Luo, X., et al. (2023). Agroecological risk assessment based on coupling of water and land resources—a case of Heihe River basin. *Land* 12 (4), 794. doi:10.3390/land12040794

Yu, T., Feng, Q., Si, J., Zhang, X., Xi, H., and Zhao, C. (2017). Comparable water use of two contrasting riparian forests in the lower Heihe River basin, Northwest China. *J. For. Res.* 29, 1215–1224. doi:10.1007/s11676-017-0540-2

Yuan, R., Li, Z., and Wang, M. (2022). Influences of overlapped riparian groundwater mounds on interaction between surface water and groundwater. *Hydrol. Process.* 36 (3). doi:10.1002/hyp.14552

Yuan, R., Wang, M., Wang, S., and Song, X. (2020). Water transfer imposes hydrochemical impacts on groundwater by altering the interaction of groundwater and surface water. *J. Hydrology* 583, 124617. doi:10.1016/j.jhydrol.2020.124617

Zeng, Y., Zhao, C., Shi, F., Schneider, M., Lv, G., and Li, Y. (2020). Impact of groundwater depth and soil salinity on riparian plant diversity and distribution in an arid area of China. *Sci. Rep.* 10 (1), 7272. doi:10.1038/s41598-020-64045-w

Zhang, H., Yu, J., Wang, P., Wang, T., and Li, Y. (2021). Groundwater-fed oasis in arid Northwest China: insights into hydrological and hydrochemical processes. *J. Hydrology* 597, 126154. doi:10.1016/j.jhydrol.2021.126154

Zhang, J., Liu, S., Wang, T., Wang, P., Yu, J., and Alatengtuya, A. (2023a). Streamflow and sediment characteristics of Ejina River under ecological water transportation. *South-to-North Water Transfers Water Sci. Technol.* 2023 (3), 531–540. doi:10.13476/j.cnki.nsbdqk.2023.0053

Zhang, X., Wang, P., Wang, T., Yu, J., and Liu, X. (2019). Relationship between chemical characteristics of shallow groundwater and water level depth in Ejina Oasis under water conveyance conditions. *South-to-North Water Transfers Water Sci. Technol.* 17 (06), 86–94. doi:10.13476/j.cnki.nsbdqk.2019.0139

Zhang, Y. (2023). Improved statistical models for the relationship between riparian vegetation and river flow in arid environments: implications for flow management. *Sci. Total Environ.* 874, 162487. doi:10.1016/j.scitotenv.2023.162487

Zhang, Y., Yu, J., Wang, P., and Fu, G. (2011). Vegetation responses to integrated water management in the Ejina basin, northwest China. *Hydrol. Process.* 25 (22), 3448–3461. doi:10.1002/hyp.8073

Zhang, Y., Zou, X., Wang, Y., Wang, J., and Li, J. (2023b). Effects of Tamarix ramosissima on the distribution of Populus euphratica in various soilwater and salinity environments in the Ejina Oasis, Inner Mongolia of northern China. *J. Beijing For. Univ.* 45 (03), 11–20.

Zhu, G. F., Li, Z. Z., Su, Y. H., Ma, J. Z., and Zhang, Y. Y. (2007). Hydrogeochemical and isotope evidence of groundwater evolution and recharge in Minqin Basin, Northwest China. *J. Hydrology* 333 (2-4), 239–251. doi:10.1016/j.jhydrol.2006.08.013

Zhu, G. F., Su, Y. H., and Feng, Q. (2008). The hydrochemical characteristics and evolution of groundwater and surface water in the Heihe River Basin, northwest China. *Hydrogeology J.* 16 (1), 167–182. doi:10.1007/s10040-007-0216-7